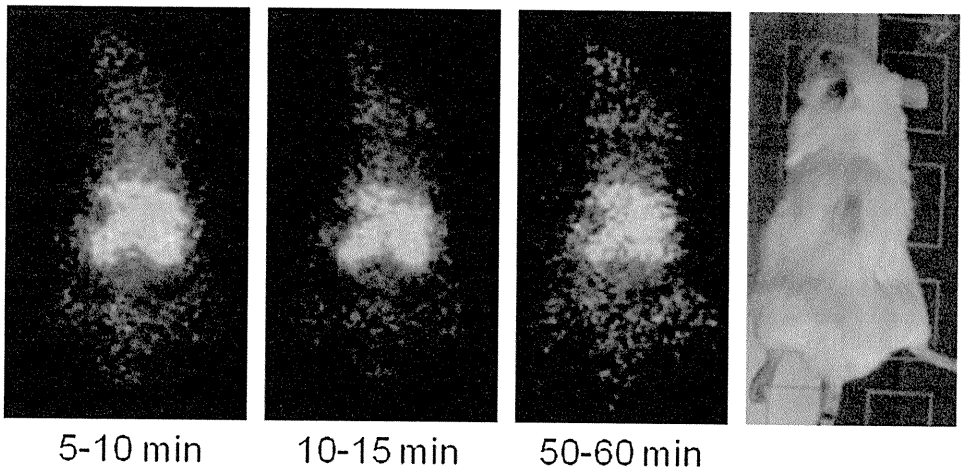

Fig. 6. Whole-body imaging of [^{11}C]IL-8 in mice with PPIS. Mice anesthetized with isoflurane were positioned prone on an acrylic plate and placed on the midplane between two opposing detectors (PPIS) arranged in a horizontal mode.

Here, we proposed a unique approach for preparing a positron-labeled peptide or protein using a positron-labeled amino acid and a cell-free translation system that contains enzymes and essential factors for protein synthesis. To prove the concept of this new approach, we tried to synthesize a positron-labeled IL-8 with easily available [^{11}C]MET and a commercially available PURESYSTEM. As the synthesis reaction proceeded very smoothly, [^{11}C]IL-8 was efficiently (63% yield) prepared within a short time (20 min) even when using [^{11}C]MET with a short half-life of 20.4 min. In addition, we succeeded in synthesizing [^{11}C]dihydrofolate reductase, a prokaryotic protein, using the PURESYSTEM and [^{11}C]MET (data not shown). As far as we know, this is the first report that a cell-free translation system can be used for synthesis of a positron-labeled protein for PET.

One of the notable features of this method is that the protein synthesis will stop when the positron-labeled amino acid is exhausted. That is, only a trace amount of positron-labeled protein is synthesized in this method because a positron-labeled amino acid is generally prepared with high specific activity by a non-carrier-added condition. Therefore, this method holds promise to prepare a positron-labeled protein with high specific activity at the same level of the positron-labeled amino acid in theory. Further study is needed for the large-scale production of carbon-11-labeled proteins using a cell-free translation system and [^{11}C] methionine. One possible approach will be the radiochemistry on microfabricated devices.

Besides facilitating the synthesis of active natural proteins, the purified protein synthesis system has many other applications due to its high controllability. Cell-free systems provide greater flexibility for incorporation of unnatural amino acids at a specific residue of a synthesized protein using a suppressor-tRNA charged chemically or enzymatically [24]. This would enable us to use a fluorine-18-labeled amino acid for preparation of a positron-labeled protein, although some unnatural amino acid cannot be recognized by a cell-free translation system. Because imaging of neutrophilic infiltration with radiolabeled IL-8 requires imaging at several hours after injection, the development of new labeling methods using fluorine-18-labeled unnatural amino acid would be a next step for this study. Although further studies are needed to improve the procedures, this labeling method using protein translation system could open up a new field of positron-labeled protein research in the future.

4. Conclusions

In summary, we investigated the use of a cell-free protein synthesis system for preparation of positron emitter-labeled protein. [^{11}C]IL-8 was synthesized using commercially available PURESYSTEM and [^{11}C]MET as an example. The in vitro synthesis proceeded very smoothly, and maximum radioactivity of [^{11}C]IL-8 was obtained within a short reaction time (20 min). In addition, purification of [^{11}C]IL-8 could be achieved easily by a simple cation exchange and ultrafiltration system, resulting in excellent radiochemical purity (>95%). This excellent radiochemical purity was sufficient for use of [^{11}C]IL-8 as a radioactive probe for PET imaging. This new method promises to be a useful tool for radiolabeling of biomolecules.

Acknowledgments

The authors appreciate Post Genome Institute Co. Ltd. (Japan) for giving precise technical information on PURESYSTEM. This work was supported by Grants-in-Aid for scientific research (nos. 21390171 and 21650088) from the Japan Society of Promotion of Science and the Ministry of Education, Culture, Sports, Science, and Technology in Japan. The authors also thank J. Tsubata, M. Kato and T. Ohnuki for their assistance.

References

[1] Shimizu Y, Kanamori T, Ueda T. Protein synthesis by pure translation systems. Methods 2005;36:299–304.

[2] Pavlou AK, Reichert JM. Recombinant protein therapeutics — success rates, market trends and values to 2010. Nat Biotechnol 2004;22: 1513–9.

[3] Brekke OH, Sandlie I. Therapeutic antibodies for human diseases at the dawn of the twenty-first century. Nat Rev Drug Discov 2003;2:52–62.

[4] Hwang DR, Evelhoch J. How the biopharmaceutical industry uses molecular imaging. J Nucl Med 2008;49:24N–5N.

[5] Levin CS. Primer on molecular imaging technology. Eur J Nucl Med Mol Imaging 2005;32(Suppl 2):S325–45.

[6] Tolmachev V, Stone-Elander S. Radiolabelled proteins for positron emission tomography: pros and cons of labelling methods. Biochim Biophys Acta 2010;1800:487–510.

[7] Malviya G, Signore A, Lagana B, Dierckx RA. Radiolabelled peptides and monoclonal antibodies for therapy decision making in inflammatory diseases. Curr Pharm Des 2008;14:2401–14.

[8] Miller PW, Long NJ, Vilar R, Gee AD. Synthesis of 11C, 18F, 15O, and 13N radiolabels for positron emission tomography. Angew Chem Int Ed Engl 2008;47:8998–9033.

[9] Heppeler A, Froidevaux S, Macke HR, Jermann E, Behe M, Powell P, et al. Radiometal-labelled macrocyclic chelator-derivatised somatostatin analogue with superb tumour-targeting properties and potential for receptor-mediated internal radiotherapy. Chem-Eur J 1999;5: 1974–81.

[10] Velikyan I, Beyer GJ, Langstrom B. Microwave-supported preparation of (68)Ga bioconjugates with high specific radioactivity. Bioconjug Chem 2004;15:554–60.

[11] Koehler L, Gagnon K, McQuarrie S, Wuest F. Iodine-124: a promising positron emitter for organic PET chemistry. Molecules 2010;15: 2686–718.

[12] Shimizu Y, Inoue A, Tomari Y, Suzuki T, Yokogawa T, Nishikawa K, et al. Cell-free translation reconstituted with purified components. Nat Biotechnol 2001;19:751–5.

[13] Van Damme J, Rampart M, Conings R, Decock B, Van Osselaer N, Willems J, et al. The neutrophil-activating proteins interleukin 8 and beta-thromboglobulin: in vitro and in vivo comparison of NH2-terminally processed forms. Eur J Immunol 1990;20:2113–8.

[14] Hebert CA, Luscinskas FW, Kiely JM, Luis EA, Darbonne WC, Bennett GL, et al. Endothelial and leukocyte forms of IL-8. Conversion by thrombin and interactions with neutrophils. J Immunol 1990;145: 3033–40.

[15] Schutyser E, Struyf S, Proost P, Opdenakker G, Laureys G, Verhasselt B, et al. Identification of biologically active chemokine isoforms from ascitic fluid and elevated levels of CCL18/pulmonary and activation-regulated chemokine in ovarian carcinoma. J Biol Chem 2002;277: 24584–93.

[16] Gross MD, Shapiro B, Fig LM, Steventon R, Skinner RW, Hay RV. Imaging of human infection with (131)I-labeled recombinant human interleukin-8. J Nucl Med 2001;42:1656–9.

[17] Bleeker-Rovers CP, Rennen HJ, Boerman OC, Wymenga AB, Visser EP, Bakker JH, et al. 99mTc-labeled interleukin 8 for the scintigraphic detection of infection and inflammation: first clinical evaluation. J Nucl Med 2007;48:337–43.

[18] Arnold K, Bordoli L, Kopp J, Schwede T. The SWISS-MODEL workspace: a web-based environment for protein structure homology modelling. Bioinformatics 2006;22:195–201.

[19] Kiefer F, Arnold K, Kunzli M, Bordoli L, Schwede T. The SWISS-MODEL repository and associated resources. Nucleic Acids Res 2009; 37:D387–92.

[20] Peitsch MC. Protein modeling by e-mail. Bio-Technology 1995;13:658–60.

[21] Pascali C, Bogni A, Iwata R, Decise D, Crippa F, Bombardieri E. High efficiency preparation of L-S-methyl-C-11 methionine by on-column C-11 methylation on C18 Sep-Pak. J Label Compd Radiopharm 1999; 42:715–24.

[22] Nagren K, Halldin C. Methylation of amide and thiol functions with C-11 methyl triflate, as exemplified by C-11 NMSP, C-11 flumazenil and C-11 methionine. J Label Compd Radiopharm 1998;41:831–41.

[23] Tsukada H, Sato K, Fukumoto D, Nishiyama S, Harada N, Kakiuchi T. Evaluation of D-isomers of O-11C-methyl tyrosine and O-18F-fluoromethyl tyrosine as tumor-imaging agents in tumor-bearing mice: comparison with L- and D-11C-methionine. J Nucl Med 2006;47:679–88.

[24] Kiga D, Sakamoto K, Kodama K, Kigawa T, Matsuda T, Yabuki T, et al. An engineered *Escherichia coli* tyrosyl-tRNA synthetase for site-specific incorporation of an unnatural amino acid into proteins in eukaryotic translation and its application in a wheat germ cell-free system. Proc Natl Acad Sci USA 2002;99:9715–20.

Ann Nucl Med (2011) 25:732–739
DOI 10.1007/s12149-011-0518-7

ORIGINAL ARTICLE

A modified method of 3D-SSP analysis for amyloid PET imaging using [^{11}C]BF-227

Tomohiro Kaneta · Nobuyuki Okamura · Satoshi Minoshima · Katsutoshi Furukawa · Manabu Tashiro · Shozo Furumoto · Ren Iwata · Hiroshi Fukuda · Shoki Takahashi · Kazuhiko Yanai · Yukitsuka Kudo · Hiroyuki Arai

Received: 23 March 2011 / Accepted: 6 July 2011 / Published online: 27 July 2011

Abstract
Objective Three-dimensional stereotactic surface projection (3D-SSP) analyses have been widely used in dementia imaging studies. However, 3D-SSP sometimes shows paradoxical results on amyloid positron emission tomography (PET) analyses. This is thought to be caused by errors in anatomical standardization (AS) based on an ^{18}F-fluorodeoxyglucose (FDG) template. We developed a new method of 3D-SSP analysis for amyloid PET imaging, and used it to analyze ^{11}C-labeled 2-(2-[2-dimethylaminothiazol-5-yl]ethenyl)-6-(2-[fluoro]ethoxy)benzoxazole (BF-227) PET images of subjects with mild cognitive impairment (MCI) and Alzheimer's disease (AD).
Methods The subjects were 20 with MCI, 19 patients with AD, and 17 healthy controls. Twelve subjects with MCI were followed up for 3 years or more, and conversion to AD was seen in 6 cases. All subjects underwent PET with both FDG and BF-227. For AS and 3D-SSP analyses of PET data, Neurostat (University of Washington, WA, USA) was used. Method 1 involves AS for BF-227 images using an FDG template. In this study, we developed a new method (Method 2) for AS: First, an FDG image was subjected to AS using an FDG template. Then, the BF-227 image of the same patient was registered to the FDG image, and AS was performed using the transformation parameters calculated for AS of the corresponding FDG images. Regional values were normalized by the average value obtained at the cerebellum and values were calculated for the frontal, parietal, temporal, and occipital lobes. For statistical comparison of the 3 groups, we applied one-way analysis of variance followed by the Bonferroni post hoc test. For statistical comparison between converters and non-converters, the t test was applied. Statistical significance was defined as $p < 0.05$.

T. Kaneta (✉) · S. Takahashi
Department of Diagnostic Radiology,
Tohoku University, 1-1 Seiryomachi, Aobaku,
Sendai 980-8574, Japan
e-mail: kaneta@rad.med.tohoku.ac.jp

N. Okamura · S. Furumoto · K. Yanai
Department of Pharmacology, Tohoku University Graduate School of Medicine, 4-1 Seiryomachi,
Aobaku, Sendai 980-8575, Japan

S. Minoshima
Department of Radiology, University of Washington,
1959 N.E. Pacific Street, Seattle, WA 98195-7115, USA

K. Furukawa · H. Arai
Division of Brain Sciences, Department of Geriatrics and Gerontology, Institute of Development, Aging and Cancer,
Tohoku University, 4-1 Seiryomachi, Aobaku,
Sendai 980-8498, Japan

M. Tashiro
Division of Cyclotron Nuclear Medicine, Cyclotron and Radioisotope Center, Tohoku University, 6-3 Aoba,
Aramaki, Aoba-ku, Sendai, Miyagi 980-8578, Japan

R. Iwata
Division of Radiopharmaceutical Chemistry, Cyclotron and Radioisotope Center, Tohoku University, 6-3 Aoba, Aramaki,
Aoba-ku, Sendai, Miyagi 980-8578, Japan

H. Fukuda
Nuclear Medicine and Radiology, Institute of Development, Aging and Cancer, Tohoku University, 4-1 Seiryomachi,
Aobaku, Sendai 980-8498, Japan

Y. Kudo
Department of NeuroImaging Research, Innovation New Biomedical Engineering Center, Tohoku University,
4-1 Seiryomachi, Aobaku, Sendai 980-8498, Japan

Results Among the 56 cases we studied, Method 1 demonstrated slight distortions after AS of the image in 16 cases and heavy distortions in 4 cases in which the distortions were not observed with Method 2. Both methods demonstrated that the values in AD and MCI patients were significantly higher than those in the controls, in the parietal, temporal, and occipital lobes. However, only Method 2 showed significant differences in the frontal lobes. In addition, Method 2 could demonstrate a significantly higher value in MCI-to-AD converters in the parietal and frontal lobes.

Conclusions Method 2 corrects AS errors that often occur when using Method 1, and has made appropriate 3D-SSP analysis of amyloid PET imaging possible. This new method of 3D-SSP analysis for BF-227 PET could prove useful for detecting differences between normal groups and AD and MCI groups, and between converters and non-converters.

Keywords 3D-SSP · Voxel-based · Amyloid · PET · BF-227

Introduction

Three-dimensional stereotactic surface projection (3D-SSP) analysis [1, 2] has been widely used in dementia imaging studies. This is a method of analysis that extracts metabolic activity from cortical gray matter after anatomical standardization (AS). By extracting the peak activity for each corresponding area of the cortex and assigning it to a surface pixel, the algorithm also can compensate for individual differences in cortical thickness and gyri depth in the standard stereotactic system. Thus, 3D-SSP is advantageous in intergroup comparisons and provides sensitive and robust results when evaluating dementing diseases [2]. However, 3D-SSP sometimes demonstrates paradoxical results on amyloid PET analyses, such as significant abnormalities in cognitively normal subjects. This is thought to be caused by AS errors. Automated AS requires a digital brain template that is matched anatomically with a standard brain atlas. 3D-SSP uses a brain template created by averaging a large number of normal ^{18}F-fluorodeoxyglucose (FDG) positron emission tomography (PET) data (FDG template) [1]. FDG accumulates mainly in the gray matter in the brain, thus showing a totally different distribution from the amyloid PET tracer. On the other hand, amyloid PET tracers, such as Pittsburgh Compound-B (PiB) [3, 4] and ^{11}C-labeled 2-(2-[2-dimethylaminothiazol-5-yl]ethenyl)-6-(2-[fluoro]ethoxy)benzoxazole (BF-227) [5, 6], often demonstrate non-specific high levels of accumulation in the white matter, more commonly in cognitively normal individuals. The FDG template therefore seems inappropriate for 3D-SSP analysis of amyloid PET images. However, a template for amyloid PET is not yet available for 3D-SSP analysis. In this study, we report the development of a new 3D-SSP analysis method for amyloid PET imaging, which solves this problem; we also describe its use in the analysis of BF-227 PET in normal subjects as well as patients with mild cognitive impairment (MCI) and Alzheimer's disease (AD).

Methods

Subjects recruited in the present study included 20 individuals with amnestic MCI, 19 patients with AD, and 17 age-matched normal controls (NC). The demographic parameters of the subjects are shown in Table 1. Among the MCI subjects, 12 were followed up for 3 years or more, and conversion to AD was seen in 6. The control group was recruited from among volunteers, none of whom were on centrally acting medication, had cognitive impairment, or had cerebrovascular lesions identified on MRI. The study protocol was approved by the Committee on Clinical Investigation at Tohoku University School of Medicine and the Advisory Committee on Radioactive Substances at Tohoku University. After describing the study to the patients and subjects, written informed consent was obtained.

All subjects underwent PET with both FDG and BF-227. BF-227 and its *N*-desmethylated derivative (a precursor of BF-227) were custom-synthesized by Tanabe R&D Service Co. BF-227 was synthesized from the precursor by *N*-methylation in dimethyl sulfoxide using [^{11}C]methyl triflate. Both FDG and BF-227 PET were performed using a PET SET-2400W scanner (Shimadzu Inc., Japan) with a spatial resolution of 4 mm (transaxial) and 4.5 mm (axial) at full-width half-maximum (FWHM) in the center of the field of view. For attenuation correction, a transmission scan was performed using ^{68}Ge/Ga sources for 7 min. The BF-227 PET scan was performed for 60 min after intravenous injection of 211–366 MBq of BF-227 with the subjects' eyes closed. The data obtained at 40–60 min after injection were used for the calculation of standardized uptake value (SUV), a tissue radioactivity concentration

Table 1 Demographic details of the subjects in this study

	N	Gender	Age	MMSE
NC	17	M/F = 7/10	67.0 ± 4.1	29.9 ± 0.3
MCI	20	M/F = 10/10	76.6 ± 4.7	25.5 ± 2.3
AD	19	M/F = 5/14	73.7 ± 7.0	20.0 ± 3.5

NC normal control, *MCI* mild cognitive impairment, *AD* Alzheimer's disease, *M* male, *F* female

normalized by injected dose and body weight. For FDG PET, subjects were scanned after at least 4 h of food restriction in a quiet and dimly lit room with their eyes closed. An emission scan was performed 60 min after intravenous injection of about 370 MBq of FDG for 10 min. The emission data were corrected for tissue attenuation on the basis of the transmission data.

Anatomical standardization of BF-227 images

Two kinds of AS for BF-227 images were performed: (1) Method 1, which performs AS for BF-227 images using an FDG template; (2) Method 2 (a new method for AS), which we have described below. First, the FDG image was subjected to AS using an FDG template. The BF-227 image was then registered to the FDG image, and AS was performed using the transformation parameters calculated for AS of the corresponding FDG images. We used the software library Neurostat (University of Washington, Seattle, WA, USA) for neurological and biomedical image analyses. The programs used in Method 2 were mainly "stereo," "coreg," and "swarpreg." "Stereo" is a program for stereotactic image registration, and creates library files containing data for linear and nonlinear transformation. In Method 2, we created these library files for FDG images, and applied them to BF-227 images. "Coreg" is a program for three-dimensional image co-registration, which we used to align BF-227 images to FDG images. Next, we used "swarpreg," which is a program for three-dimensional stereotactic image warping for BF-227 images that uses library files for FDG images. A combination of these procedures enabled the transformation of individual BF-227 images into the stereotactic space of the standard brain.

Analysis

Regional values were extracted from cortical gray matter to the surface of the template by the 3D-SSP method in the same manner as FDG PET, and were normalized by the extracted value from the cerebellar gray matter (eSUVR). The values were calculated for the frontal, parietal, temporal, and occipital lobes using "sspvoiclassic" program in Neurostat. The right and left lobes of each subject were analyzed evenly. For statistical comparison between the 3 groups, we applied one-way analysis of variance followed by the Bonferroni post hoc test. For statistical comparison between converters and non-converters, the t test was applied. Statistical significance was defined as $p < 0.05$.

For voxel-based comparison with normal subjects, normal databases were created by averaging the images from NC after AS by Method 1 and 2, individually. The 3D-SSP z-map images were normalized to those of the cerebellum, and were shown within the range of 1–5 of the z score.

For voxel-based two-sample comparison, t test was applied. Z scores were calculated using "ssp2tz" program in Neurostat. The 3D-SSP z-map images were shown within the range of 1–5 of the z score.

Results

Case presentation

The patient was an 81-year-old woman with a diagnosis of MCI. The mini-mental state examination (MMSE) score was 26. FDG PET did not demonstrate an AD-like pattern, which is characterized by decreased uptake at the parietal lobe or posterior cingulate gyrus (Fig. 1a). BF-227 PET did not demonstrate significantly increased uptake in the brain (Fig. 1b). However, 3D-SSP results analyzed by Method 1 showed significant generalized abnormalities in the brain, suggesting AD (Fig. 1c). On the other hand, those analyzed by Method 2 did not demonstrate such abnormalities (Fig. 1d). This patient was followed up for over 3 years, but did not convert to AD. Figure 1e shows the BF-227 image after AS by Method 1, showing considerable distortions, mainly in the frontal lobes. The BF-227 image after AS by Method 2 did not show such distortions (Fig. 1f).

Anatomical standardization

When a total of 56 cases were analyzed by both methods, Method 1 demonstrated 17 cases with slightly distorted images and 4 cases with heavily distorted images after AS. Table 2 shows the cases with such distortions after Method 1. These distortions were mainly seen at the frontal lobes with angular deformity, and were seen uniformly among subjects with AD, MCI, and NC. On the other hand, analysis by Method 2 did not show such distortions, and AS was successful in these cases (Fig. 1). However, scan failure in one case and an error in the registration of the BF-227 image to the FDG image in another case necessitated their exclusion from subsequent analyses.

Regional analyses

The regional analyses demonstrated that the mean values for the AD, MCI, and NC groups by Method 1 were in the range 1.05–1.09, 1.01–1.05, and 0.96–0.98, respectively, while they were found to be 1.08–1.12, 1.06–1.10, and 0.96–1.00, respectively, by Method 2. Method 2 demonstrated significant differences between AD and NC, and

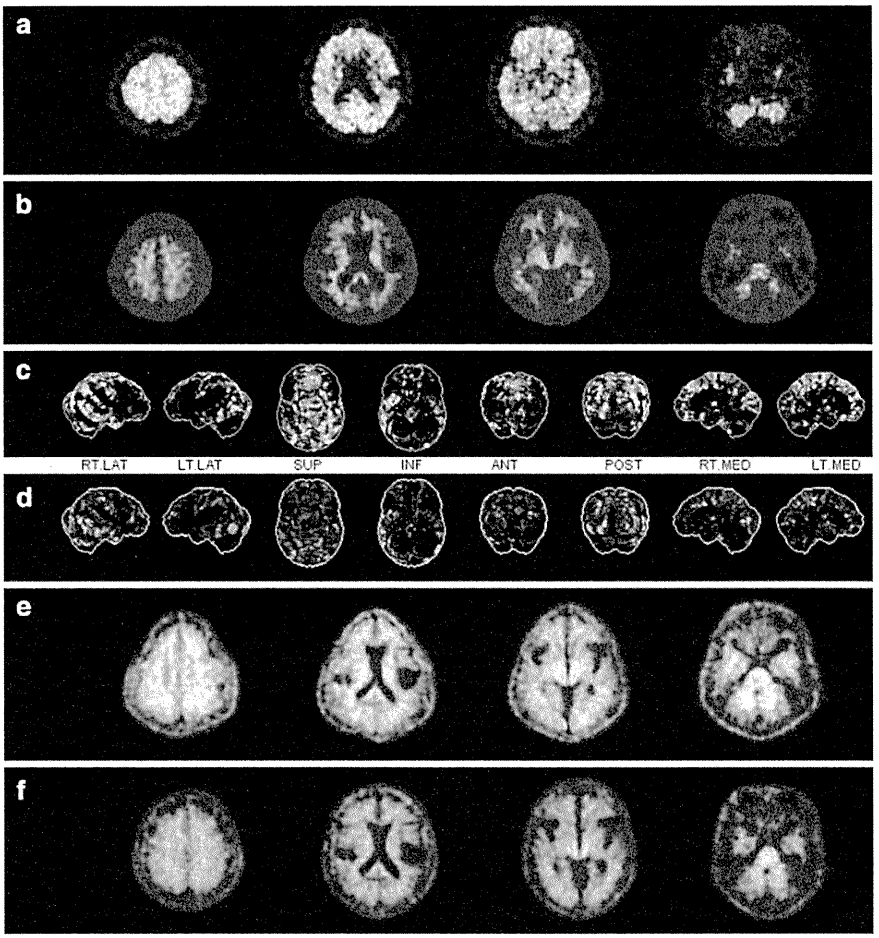

Fig. 1 An 81-year-old female with a diagnosis of MCI (MMSE was 26). **a** FDG PET did not demonstrate an AD pattern. **b** BF-227 PET did not demonstrate significantly increased uptake in the brain. **c** 3D-SSP results by Method 1 showed generalized significant abnormalities in the brain suggesting AD, although **d** those analyzed by Method 2 did not. This patient was followed up for 3 years, but did not convert to AD. **e** BF-227 images after co-registration to FDG images by Method 1. The distortions were seen mainly in the frontal lobes. **f** BF-227 images after co-registration to FDG images by Method 2. No distortions were seen

Table 2 The numbers of cases with distortions after Method 1

	AD	MCI	NC	Total
Slight	6	5	6	17
Strong	1	2	1	4
Total	7	7	7	21

A sample of anatomically standardized image with slight distortion.

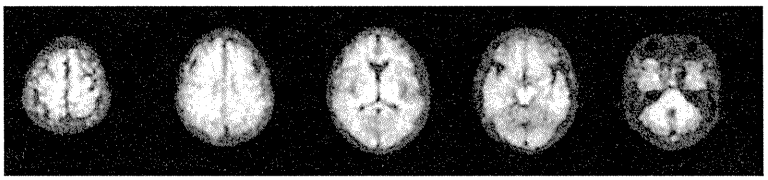

A sample of anatomically standardized image with strong distortion.

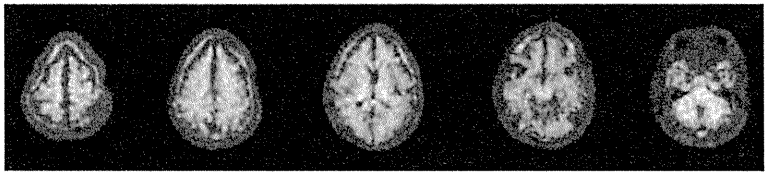

between MCI and NC in all the lobes, but Method 1 did not show a significant difference between MCI and NC in the frontal lobe (Fig. 2).

Method 2 demonstrated that converters showed significantly higher values than non-converters in the parietal and frontal lobes, which was not observed with Method 1 (Fig. 3).

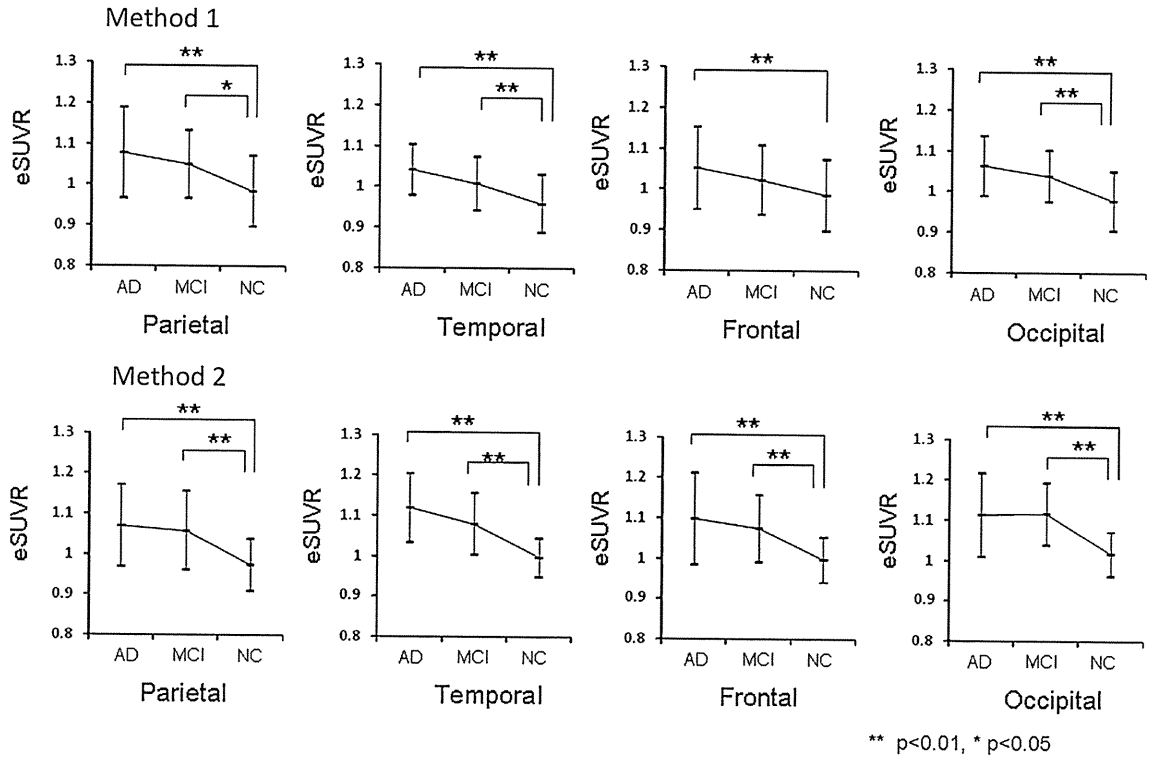

Fig. 2 Mean (SD) of eSUVR in the AD, MCI, and control groups calculated by Method 1 and 2. The values were calculated for the parietal, temporal, frontal, and occipital lobes

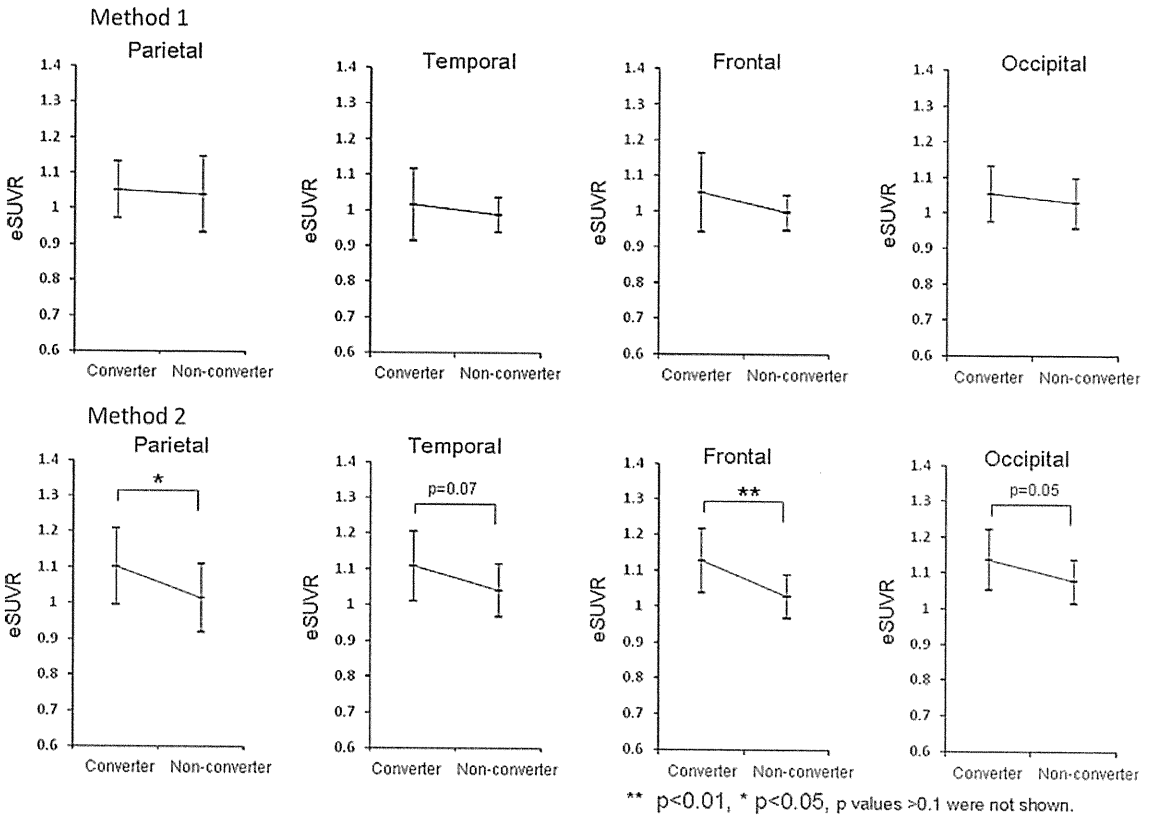

Fig. 3 Mean (SD) of eSUVR for MCI-to-AD converters and non-converters calculated by Method 1 and 2. The values were calculated for the parietal, temporal, frontal, and occipital lobes

3D-SSP analyses

Figure 4 a–c shows the *Z* score maps of 3D-SSP analyses processed by Method 1 and 2, comparing AD and NC, MCI and NC, and converters and non-converters. The differences between Method 1 and 2 were not clear in Fig. 4a, b; however, Fig. 4c demonstrated more intense and widespread abnormalities between converters and non-converters by Method 2 than by Method 1.

Figure 5 a–c shows the *Z* score maps processed by Method 2 comparing converters and NC, non-converters and NC, and converters and non-converters, respectively. Figure 5a reveals a similar distribution to that in Fig. 4a, b, but with the scores slightly higher than those in Fig. 4b and slightly lower than those in Fig. 4a. Figure 5b showed a globally low *z* score that was slightly higher in the left temporal lobe. Figure 5c demonstrated differences between converters and non-converters especially in both lateral frontal lobes.

Discussion

Voxel-based analysis allows an objective and sensitive identification of regional changes. Statistical parametric mapping (SPM) [7] and 3D-SSP have both been commonly used for voxel-based analysis for brain PET and SPECT. However, for amyloid PET analysis, most researchers have performed SPM analyses using an MR template after registration of PET images to MR images [8, 9]. In this case, the AS of SPM will not be influenced by the distribution of PET tracers. 3D-SSP can also utilize MR images, but this method is not commonly performed. The 3D-SSP analysis of amyloid PET images using an FDG template entails the problems mentioned in "Introduction". In fact, our results demonstrated that Method 1 showed varying degrees of errors for AS in 38% of the cases. These errors may not only produce an overestimation or underestimation of the amyloid burden in the brain, but also result in the creation of inaccurate normal databases for voxel-based analysis. Thus, Method 1 seems inappropriate for 3D-SSP analysis of amyloid PET. FDG PET has been widely accepted as the method to assess functional abnormalities in dementia [10–12], and is commonly used for clinical evaluation of patients with MCI and AD. Most of those who underwent amyloid PET have also undergone FDG PET. We proposed to take advantage of this coupling of PET images to solve the problem of 3D-SSP analysis for amyloid PET. Although this problem has been noticed by some researchers, to our knowledge, this is the first paper to demonstrate this problem and present a solution.

For AS of the brain images, a standard stereotactic atlas brain (template) is necessary. Although templates differ to some degree between software programs, a template is basically created by averaging a large number of normal scans. In addition, Neurostat uses hundreds of predefined landmarks for nonlinear warping [1]. It seemed difficult to create an original template with landmarks for amyloid PET by ourselves. Therefore, the next step was to utilize an FDG template after co-registration of FDG and BF-227 images. Because these images are obtained from the same subjects, it is possible to register them accurately using linear transformation methods, such as translocations and rotations. For the registration criterion, Neurostat uses mutual information (MI). The MI of the image intensity values of corresponding voxel pairs is maximal if the images are geometrically aligned. Because no assumptions are made regarding the nature of the relation between the image intensities in both modalities, this criterion is very general and powerful and can be applied automatically without prior segmentation to a large variety of techniques [13–16]. After the registration, Neurostat successfully warped registered BF-227 images using transformation parameters calculated for the AS of corresponding FDG images.

Results of regional analysis demonstrated that both Method 1 and 2 showed significantly higher uptake in AD and MCI patients compared to NC subjects for most lobes, but Method 1 did not show significant differences between MCI and NC subjects for the frontal lobe. In addition, only Method 2 demonstrated significant differences between converters and non-converters. These differences were also obvious on 3D-SSP results when Method 2 was used. Because BF-227 is thought to have lower sensitivity for diffuse amyloid plaques, and a higher sensitivity for neuritic plaques than PiB, BF-227 has been reported to have potential as a method for predicting the conversion from MCI to AD accurately [6, 17, 18]. Previous regions-of-interest analyses for almost same subjects with this study demonstrated that increased BF-227 retention was evident in both the converters and AD patients, but not in the control subjects or the non-converters [17]. Considering these facts, Method 2 seems to provide more sensitive and accurate results than Method 1. In addition, 3D-SSP results subjected to Method 2 showed preferential accumulation in the temporal lobes, supporting previous reports that used SPM [19].

The new method, however, has some limitations. First, it requires successful FDG scans. If an FDG image has problems, Method 2 cannot be applied to it. Another problem with Method 2 is the possible creation of errors by misregistration of amyloid images. While the reason for this is not clear, it has been reported that standardization by 3D-SSP was not accurate enough at a head tilt of approximately 25° or more [20]. It is thus important to check each image after registration and AS.

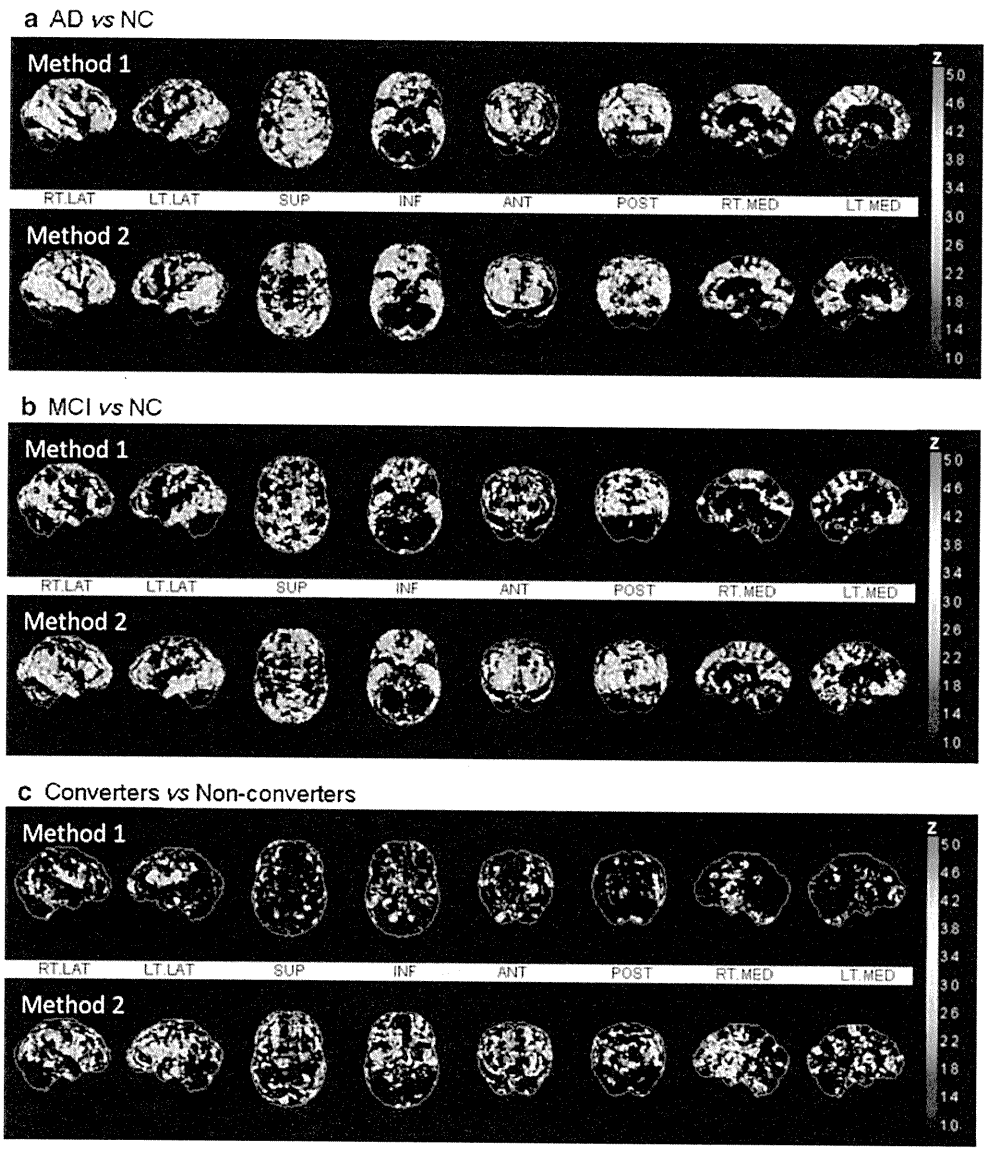

Fig. 4 *Z* score maps of 3D-SSP analyses processed by Method 1 and 2 of the **a** AD group compared to NC group, the **b** MCI group compared to NC group, and **c** converters compared to non-converters

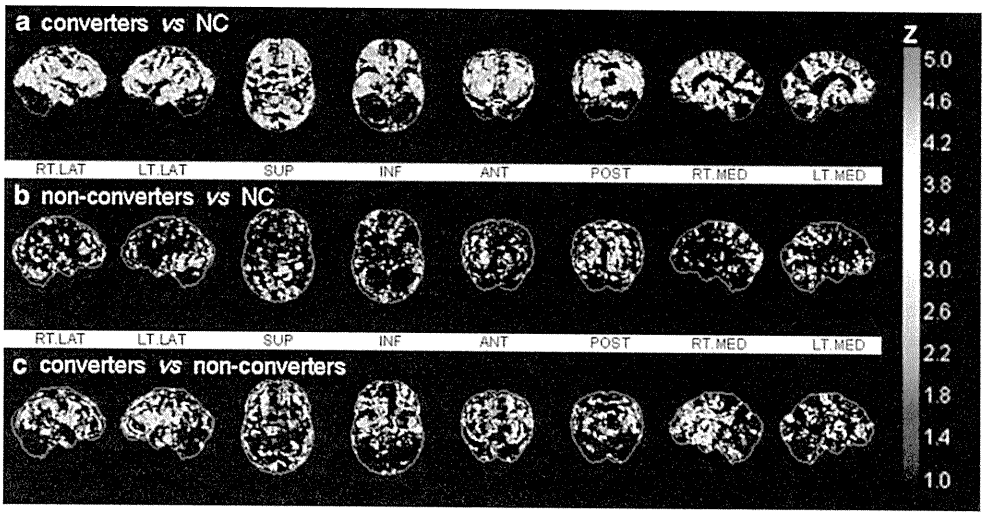

Fig. 5 *Z* score maps processed by Method 2 of **a** converters compared to NC group, **b** non-converters compared to NC group, and **c** converters compared to non-converters

We would like to conclude that our newly developed method can be used to modify errors in 3D-SSP analyses of amyloid PET imaging. 3D-SSP analysis of BF-227 PET was useful for detecting differences between AD and NC groups, MCI and NC groups, and converters and non-converters. Further investigation is required for the evaluation of the utility for individual differentiations.

Acknowledgments We appreciate the technical assistance provided by Seiichi Watanuki of CYRIC in Tohoku University (Sendai, Japan) and Frank Thiele of Philips Research North America (NY, USA).

Sources of funding for the article None.

References

1. Minoshima S, Koeppe RA, Frey KA, Kuhl DE. Anatomic standardization: linear scaling and nonlinear warping of functional brain images. J Nucl Med. 1994;35:1528–37.
2. Minoshima S, Frey KA, Koeppe RA, Foster NL, Kuhl DE. A diagnostic approach in Alzheimer's disease using three-dimensional stereotactic surface projections of fluorine-18-FDG PET. J Nucl Med. 1995;36:1238–48.
3. Klunk WE, Engler H, Nordberg A, Wang Y, Blomqvist G, Holt DP, et al. Imaging brain amyloid in Alzheimer's disease with Pittsburgh Compound-B. Ann Neurol. 2004;55:306–19.
4. Nordberg A. PET imaging of amyloid in Alzheimer's disease. Lancet Neurol. 2004;3:519–27.
5. Kudo Y. Development of amyloid imaging PET probes for an early diagnosis of Alzheimer's disease. Minim Invasive Ther Allied Technol. 2006;15:209–13.
6. Kudo Y, Okamura N, Furumoto S, Tashiro M, Furukawa K, Maruyama M, et al. 2-(2-[2-Dimethylaminothiazol-5-yl]ethenyl)-6-(2-[fluoro]ethoxy)benzoxazole: a novel PET agent for in vivo detection of dense amyloid plaques in Alzheimer's disease patients. J Nucl Med. 2007;48:553–61.
7. Friston KJ, Holmes AP, Worsley KJ, Poline JB, Frith C, Frackowiak RSJ. Statistical parametric maps in functional imaging: a general linear approach. Hum Brain Mapp. 1995;2:189–210.
8. Mikhno A, Devanand D, Pelton G, Cuasay K, Gunn R, Upton N, et al. Voxel-based analysis of 11C-PIB scans for diagnosing Alzheimer's disease. J Nucl Med. 2008;49:1262–9.
9. Ziolko SK, Weissfeld LA, Klunk WE, Mathis CA, Hoge JA, Lopresti BJ, et al. Evaluation of voxel-based methods for the statistical analysis of PIB PET amyloid imaging studies in Alzheimer's disease. Neuroimage. 2006;33:94–102.
10. de Leon MJ, Convit A, Wolf OT, Tarshish CY, DeSanti S, Rusinek H, et al. Prediction of cognitive decline in normal elderly subjects with 2-[(18)F]fluoro-2-deoxy-D-glucose/positron-emission tomography (FDG/PET). Proc Natl Acad Sci. 2001;98:10966–71.
11. Minoshima S, Giordani B, Berent S, Frey KA, Foster NL, Kuhl DE. Metabolic reduction in the posterior cingulate cortex in very early Alzheimer's disease. Ann Neurol. 1997;42:85–94.
12. Mosconi L, De Santi S, Li Y, Li J, Zhan J, Tsui WH, et al. Visual rating of medial temporal lobe metabolism in mild cognitive impairment and Alzheimer's disease using FDG-PET. Eur J Nucl Med Mol Imaging. 2006;33:210–21.
13. Maes F, Collignon A, Vandermeulen D, Marchal G, Suetens P. Multimodality image registration by maximization of mutual information. IEEE Trans Med Imaging. 1997;16:187–98.
14. Maes F, Vandermeulen D, Suetens P. Comparative evaluation of multiresolution optimization strategies for multimodality image registration by maximization of mutual information. Med Image Anal. 1999;3:373–86.
15. Pluim JP, Maintz JB, Viergever MA. Image registration by maximization of combined mutual information and gradient information. IEEE Trans Med Imaging. 2000;19:809–14.
16. Pluim JP, Maintz JB, Viergever MA. Mutual-information-based registration of medical images: a survey. IEEE Trans Med Imaging. 2003;22:986–1004.
17. Waragai M, Okamura N, Furukawa K, Tashiro M, Furumoto S, Funaki Y, et al. Comparison study of amyloid PET and voxel-based morphometry analysis in mild cognitive impairment and Alzheimer's disease. J Neurol Sci. 2009;285:100–8.
18. Furukawa K, Okamura N, Tashiro M, Waragai M, Furumoto S, Iwata R, et al. Amyloid PET in mild cognitive impairment and Alzheimer's disease with BF-227: comparison to FDG-PET. J Neurol. 2010;257:721–7.
19. Shao H, Okamura N, Sugi K, Furumoto S, Furukawa K, Tashiro M, et al. Voxel-based analysis of amyloid positron emission tomography probe [C]BF-227 uptake in mild cognitive impairment and alzheimer's disease. Dement Geriatr Cogn Disord. 2010;30:101–11.
20. Onishi H, Matsutake Y, Kawashima H, Matsutomo N, Amijima H. Comparative study of anatomical normalization errors in SPM and 3D-SSP using digital brain phantom. Ann Nucl Med. 2011;25:59–67.

Neuroscience 180 (2011) 305–313

YOKUKANSAN, A TRADITIONAL JAPANESE MEDICINE, AMELIORATES MEMORY DISTURBANCE AND ABNORMAL SOCIAL INTERACTION WITH ANTI-AGGREGATION EFFECT OF CEREBRAL AMYLOID β PROTEINS IN AMYLOID PRECURSOR PROTEIN TRANSGENIC MICE

H. FUJIWARA,[a] S. TAKAYAMA,[a] K. IWASAKI,[a,b]* M. TABUCHI,[c] T. YAMAGUCHI,[c] K. SEKIGUCHI,[c] Y. IKARASHI,[c] Y. KUDO,[d] Y. KASE,[c] H. ARAI[e] AND N. YAEGASHI[a]

[a]*Department of Traditional Asian Medicine, Tohoku University Graduate School of Medicine, 2-1 Seiryo-machi, Aoba-ku, Sendai 980-8574, Japan*

[b]*Center for Traditional Asian Medicine, Nishitaga National Hospital, 2-11-11 Kagitorihonco, Sendai 982-8555, Japan*

[c]*Tsumura Research Laboratories, Tsumura & Co., 3586 Yoshiwara, Ami-machi, Inashiki-gun, Ibaraki 300-1192, Japan*

[d]*Innovation of Biomedical Engineering Center, Tohoku University, 1-1 Seiryo-machi, Aoba-ku, Sendai 980-8574, Japan*

[e]*Department of Geriatrics and Gerontology, Division of Brain Sciences, Institute of Development, Aging and Cancer, Tohoku University, 4-1 Seiryo-machi, Aoba-ku, Sendai 980-8575, Japan*

Abstract—The deposition of amyloid β protein (Aβ) is a consistent pathological hallmark of Alzheimer's disease (AD) brains. Therefore, inhibition of Aβ aggregation in the brain is an attractive therapeutic and preventive strategy in the development of disease-modifying drugs for AD. An *in vitro* study demonstrated that yokukansan (YKS), a traditional Japanese medicine, inhibited Aβ aggregation in a concentration-dependent manner. An *in vivo* study demonstrated that YKS and Uncaria hook (UH), a constituent of YKS, prevented the accumulation of cerebral Aβ. YKS also improved the memory disturbance and abnormal social interaction such as increased aggressive behavior and decreased social behavior in amyloid precursor protein transgenic mice. These results suggest that YKS is likely to be a potent and novel therapeutic agent to prevent and/or treat AD, and that this may be attributed to UH.

Key words: Alzheimer's disease, aggression, amyloid β proteins, traditional medicine, Uncaria hook, yokukansan.

Alzheimer's disease (AD), the most prevalent cause of dementia, is characterized by loss of memory and cognition in the elderly. One of the pathological characteristics of AD is the progressive deposition of insoluble amyloid β protein (Aβ) as a form of senile plaques (Wirths et al., 2004). This protein comprises peptides of approximately 39–43 amino acid residues derived from the transmembrane amyloid precursor protein (APP) (Selkoe, 2002). Aβ can exist as monomers and form a variety of different aggregate morphologies including dimers, small soluble oligomers, protofibrils, diffuse plaques, and the fibrillar deposits seen in senile plaques. Protofibrils, diffuse plaques, and fibrillar deposits seem to have a predominant β-sheet structure (Tierney et al., 1988; Barrow and Zagorski, 1991), while oligomers are believed to be more globular (Barghorn et al., 2005). Abundant evidence showing that formation of these aggregates causes primary neurodegeneration in AD has led to the amyloid hypothesis, which states that the accumulation of Aβ in the CNS is highly neurotoxic and degrades synaptic function (Selkoe, 2002; Wirths et al., 2004). Therefore, it is hypothesized that the formation, deposition, and aggregation of Aβ in the brain should be primary targets for amelioration of dementia. Currently, drugs available for dementia such as acetylcholinesterase inhibitors exert only a temporary effect on cognitive dysfunction (Millard and Broomfield, 1995; Park et al., 2000; Darreh-Shori et al., 2004), and they do not prevent or reverse the formation of Aβ deposits. Among the potentially promising strategies for developing more effective anti-dementia drugs are the inhibition of Aβ fibril formation, destabilization of aggregated Aβ, or a combination of both.

In patients with AD, not only core symptoms such as cognitive impairment, but also behavioral and psychological symptoms of dementia (BPSD) such as aggression, anxiety, and hallucinations often emerge. BPSD is a serious problem for caregivers, and because its severity and the care burden show a positive correlation, therapy for BPSD is considered to be as important as therapy for the core symptoms (Nagaratnam et al., 1998; Tanji et al., 2005). To date, anti-psychotic medicines have been used for treatment of BPSD. However, the drugs induce extrapyramidal symptoms and other adverse events, and in consequence, they decrease the quality of life and increase the difficulty of maintaining activities of daily living. Thus, new remedies without adverse effects have been sought.

Herbal remedies are used worldwide and have a long history of use to alleviate a variety of symptoms of many

*Correspondence to: K. Iwasaki, Center for Traditional Asian Medicine, Nishitaga National Hospital, 2-11-11 Kagitorihonco, Sendai City 982-8 555, Miyagi Pref., Japan. Tel: +81-22-717-7185; fax: +81-22-717-7186.
E-mail address: QFG03604@nifty.com (K. Iwasaki).

Abbreviations: AD, Alzheimer's disease; APP, amyloid precursor protein; Aβ, amyloid β protein; BPSD, behavioral and psychological symptoms of dementia; DLB, dementia with Lewy bodies; TBS, tris–buffered saline; Tg(+), transgenic; Tg(−), non-transgenic; UH, Uncaria hook; YKS, yokukansan.

0306-4522/11 $ - see front matter
doi:10.1016/j.neuroscience.2011.01.064

different conditions and diseases. Recently, clinical trials in patients with AD have also shown that some traditional Japanese medicines called kampo improved Mini-Mental State Examination scores (Iwasaki et al., 2004) and blood flow in the cerebral cortex (Maruyama et al., 2006). We have reported that several traditional herbal medicines such as kamiuntanto (*Formula lienalis angelicae compositae*) (Wang et al., 2000; Nakagawasai et al., 2004) and hachimijiogan (*Pilulae octo-medicamentorum rehmanniae*) (Iwasaki et al., 2004) ameliorated symptoms of dementia.

Yokukansan (YKS, *Pulvis depressionis hepatis*) is a traditional Japanese medicine approved by the Ministry of Health, Labour and Welfare of Japan as a remedy for neurosis, insomnia, and irritability in children. Recently, we reported that it improved such BPSD as hallucinations, agitation, and aggression in patients with Alzheimer's disease, dementia with Lewy bodies (DLB), and other forms of senile dementia (Iwasaki et al., 2005a,b). Recently, to clarify the improving effect of YKS, various basic studies have been performed (Ikarashi et al., 2009; Kawakami et al., 2009, 2010; Terawaki et al., 2010). We also previously demonstrated that Uncaria hook (UH), a constituent herb of YKS, inhibited Aβ aggregation *in vitro* (Fujiwara et al., 2006), suggesting that YKS containing UH may possess anti-aggregation activity toward Aβ, and that it may improve memory disturbance and BPSD. However, sufficient animal experiments to confirm this hypothesis have not been performed yet.

The APP transgenic [Tg(+)] mouse expressing the human form of APP695SWE is known as a model of AD. Aβ accumulates in the brain of the mice with aging (Hsiao et al., 1996; Ikarashi et al., 2004). In addition, not only cognitive dysfunction but also BPSD-like symptoms such as disinhibition, hyperactivity, and impulsive behavior have been observed in Tg(+) mice (Lalonde et al., 2003; Stackman et al., 2003; Ognibene et al., 2005; Dong et al., 2005; Adriani et al., 2006; Quinn et al., 2007). These findings suggest that the Tg(+) mouse is a valuable tool for developing new drugs for dementia and BPSD.

To clarify the hypothesis described above, in the present study, we first examined the effect of YKS on Aβ aggregation *in vitro* as well as UH. Next, the effects of YKS and UH on accumulation of Aβ in the brain and phenotypes such as memory disturbance and BPSD-like behaviors such as the increase in aggressive behavior and decrease in social behavior in the Tg(+) mice were investigated.

EXPERIMENTAL PROCEDURES

Animals

Male APP Tg(+) mice, who overexpress a 695-amino acid splice form (Swedish mutation K670N M671I) of the human amyloid β precursor protein (APP695), and non-transgenic [Tg(−)] mice were purchased from Taconic Farms Inc. (Germantown, NY, USA). Each animal was housed individually in a plastic cage (230×155×155 mm^3) and allowed free access to water and standard laboratory food in a facility with the temperature controlled at 24±1 °C and relative humidity at 55±5% and with lights on from 7:00 to 19:00 h daily until the animals were used in the experiments. Experimental protocols were approved by the Animal Care and Use Committee of Tohoku University Graduate School of Medicine and complied with the procedures outlined in the Guide for the Care and Use of Laboratory Animals of Tohoku University.

Drugs and reagents

YKS is composed of seven dried medicinal herbs: *Atractylodes lancea* rhizome (4.0 g, rhizome of *Atractylodes lancea* De Candolle), Poria sclerotium (4.0 g, sclerotium of *Poria cocos* Wolf), Cnidium rhizoma (3.0 g, rhizome of *Cnidium officinale* Makino), Japanese Angelica root (3.0 g, root of *Angelica acutiloba* Kitagawa), Bupleurum root (2.0 g, root of *Bupleurum falcatum* Linné), glycyrrhiza (1.5 g, root and stolon of *Glycyrrhiza uralensis* Fisher), and UH (3.0 g, thorn of *Uncaria rhynchophylla* Miquel). The dry powdered extracts of YKS and UH were supplied by Tsumura & Co. (Tokyo, Japan).

Aβ peptides (1-40 and 1-42) and thioflavin-T were obtained from the Peptide Institute (Osaka, Japan) and Sigma (St. Louis, MO, USA), respectively. Other reagents (analytical grade) used for analysis were purchased from commercial sources.

In vitro study to evaluate effect of YKS on Aβ aggregation

Measurement of thioflavin-T to evaluate Aβ aggregation was performed using the method described by Suemoto et al. (2004) with slight modifications. Aβ (20 μM) dissolved in 50 mM potassium phosphate buffer (pH 7.4) with YKS was incubated at 37 °C for 96 h (A$\beta_{1\text{-}40}$) or 24 h (A$\beta_{1\text{-}42}$). At the end of the incubation, 3 μM thioflavin-T dissolved in 100 mM glycine buffer (pH 8.5) was added to the mixture. After incubation for 30 min at room temperature, the fluorescence of thioflavin-T bound to Aβ aggregates was measured using a microplate reader (Spectramax Gemini XS, Molecular Devices, Sunnyvale, CA, USA) with excitation at 442 nm and emission at 485 nm. The percentage inhibition was calculated by comparing the fluorescence values of test samples with those of control solutions without YKS.

In vivo study to evaluate behaviors and accumulation of Aβ

Ten-month-old Tg(+) mice were randomly divided into five groups: Tg(+) (n=10), Tg(+)+0.3% YKS (n=10), Tg(+)+1.0% YKS (n=10), Tg(+)+0.1% UH (n=10), and Tg(+)+1.0% UH (n=10). Tg(−) mice (n=10) were set as the control group. The mice in both the Tg(−) and Tg(+) groups were given normal powdered chow for 5 months from 10 to 15 months old. The mice in the Tg(+)+0.3% YKS and Tg(+)+1.0% YKS groups were given the powdered chow including 0.3% or 1.0% of YKS for 5 months. The mice in the Tg(+)+0.1% UH and Tg(+)+1.0% UH groups were given the powdered chow including 0.1% or 1.0% of UH for 5 months.

Step-through passive-avoidance tests were performed to evaluate learning ability from the age of 11 months to 14 months. Social interaction tests were performed at the age of 15 months. All behavioral tests were performed between 10:00 and 17:00 h.

After completion of behavioral tests, all mice were decapitated, and the dissected cerebral cortex was used for determination of Aβ levels.

Step-through passive-avoidance test

The apparatus (TK402D model, Neuroscience, Inc., Tokyo, Japan) for the step-through passive-avoidance test consisted of two compartments, one illuminated [100×120×100 mm^3; light at the top of compartment (27 W, 3000 lx)] and the other dark (100×170×100 mm^3). The compartments were separated by a guillotine door. During the learning stage, a mouse was placed in the illuminated safe compartment. While this compartment was lit,

the mouse stepped through the opened guillotine door into the dark compartment. The time spent in the illuminated compartment was defined as the latency period. 3 s after the mouse entered the dark compartment, a foot shock (0.01 mA, 200 V, 50 Hz ac, for 1 s) was delivered to the floor grid in the dark compartment. The mouse could escape from the shock only by stepping back into the safe illuminated compartment. Such acquisition trials during the learning stage were carried out once a day for 5 days. The mouse was judged to have learned avoidance from the foot shock when the latency period reached 300 s. Retention trials were carried out once per week for 78 days (11–14-months-old) to evaluate the retention of avoidance memory. The latency was measured for up to 300 s without delivering a foot shock. It was judged that the mouse retained the avoidance memory when it stayed in the illuminated safe compartment for 300 s.

Social interaction test

Social interaction such as aggressive behavior and social behavior in mice were evaluated by a social interaction test (File, 1980) using a square box-type open-field apparatus (50×50×40 cm^3, Neuroscience, Inc., Tokyo, Japan). A video camera was mounted vertically over the apparatus. Two mice in each group were placed together in the open-field apparatus. The interactive behaviors between the two animals were monitored by the video camera for 10 min, and the behavioral data were saved directly on a computer. Then, the total number of aggressive behaviors (tail rattling, chasing, and attacking) as the index of aggressiveness or normal social behaviors (sniffing, following, and contacting) as the index of sociability of each animal was counted by two observers blind to the treatment. The total distance traveled (cm) of each animal was analyzed as motor activity by using software (analyzing behavior system, Viewer II, Bioserve, Bonn, Germany).

Measurement of brain Aβ levels

The dissected cerebral cortex was homogenized and sonicated in Tris–buffered saline (TBS) and 70% formic acid containing 1× protease inhibitor mixtures to obtain soluble and insoluble fractions with slight modification of the method described previously (Calon et al., 2004). The homogenate was subjected to ultracentrifugation at 200,000×g at 4 °C for 20 min. The soluble supernatant was collected and frozen. To analyze the insoluble Aβ, the insoluble pellet was sonicated in 200 μl of 70% formic acid and subjected to ultracentrifugation at 300,000×g at 4 °C for 30 min to collect the soluble supernatant.

Brain $A\beta_{1-40}$ and $A\beta_{1-42}$ levels were measured using sandwich ELISA with a Human β Amyloid ELISA Kit (Wako Pure Chemical Industries, Ltd, Osaka, Japan) according to the manufacturer's instructions. BAN50 is a monoclonal antibody raised against a synthetic peptide of human $A\beta_{1-16}$; it preferentially reacts with the N-terminal portion of human Aβ starting at Asp-1, but does not cross-react with N-terminal–truncated Aβ or with rodent-type Aβ. BA27 and BC05, which specifically recognize the C terminus of $A\beta_{1-40}$ and $A\beta_{1-42}$, respectively, were conjugated with horseradish peroxidase and used as detector antibodies. The insoluble mouse brain fractions described above were neutralized and subjected to BAN50/BA27 or BAN50/BC05 ELISA. The protein concentration of the fraction was measured using a protein assay kit (Bio-Rad Lab., Hercules, CA, USA). Finally, the Aβ value was expressed as pmol per g of protein.

Data analysis

Data are expressed as mean±SEM. The date of passive-avoidance test was evaluated by analysis of variance (Kruskal-Wallis) followed by a Mann-Whitney *U* test. The data of other experiments were evaluated by one-way analysis of variance (ANOVA) followed by Bonferroni/Dunn tests. The significance level in each statistical analysis was accepted at $P<0.05$.

RESULTS

Effects of YKS on Aβ aggregation *in vitro*

The effects of YKS on $A\beta_{1-40}$ and $A\beta_{1-42}$ aggregation *in vitro* are shown in Fig. 1A, B, respectively. YKS inhibited the aggregation of $A\beta_{1-40}$ and $A\beta_{1-42}$ in a concentration-dependent manner. Significant inhibition was observed at 10 and 100 μg/ml for $A\beta_{1-40}$ and at 100 μg/ml for $A\beta_{1-42}$.

Effects of YKS and UH on memory disturbance in Tg(+) mice

Step-through passive-avoidance tests were carried out on mice at 11–14 months of age. In the first acquisition trial of the learning stage, all mice (11 months old) in the Tg(−), Tg(+), Tg(+)+YKS, and Tg(+)+UH groups entered the dark compartment immediately after being placed in the illuminated compartment. Repeating the acquisition trial increased the latency times in all groups. All mice in all

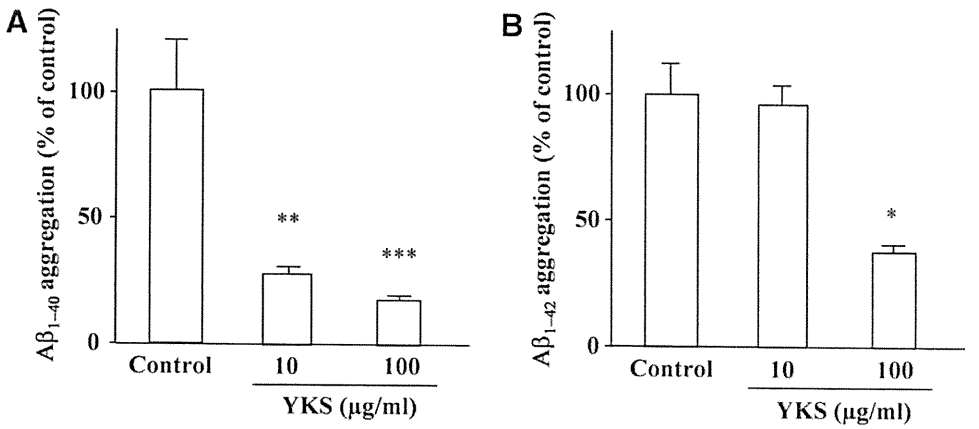

Fig. 1. Effects of YKS on $A\beta_{1-40}$ (A) or $A\beta_{1-42}$ (B) aggregation. Aβ aggregation was assessed by the thioflavin T method and expressed as the percentage of control aggregation in the absence of YKS. Values represent mean±SE from four independent experiments. Significance by Bonferroni/Dunn tests following one-way ANOVA is indicated as * $P<0.05$, ** $P<0.01$, *** $P<0.001$ vs. control.

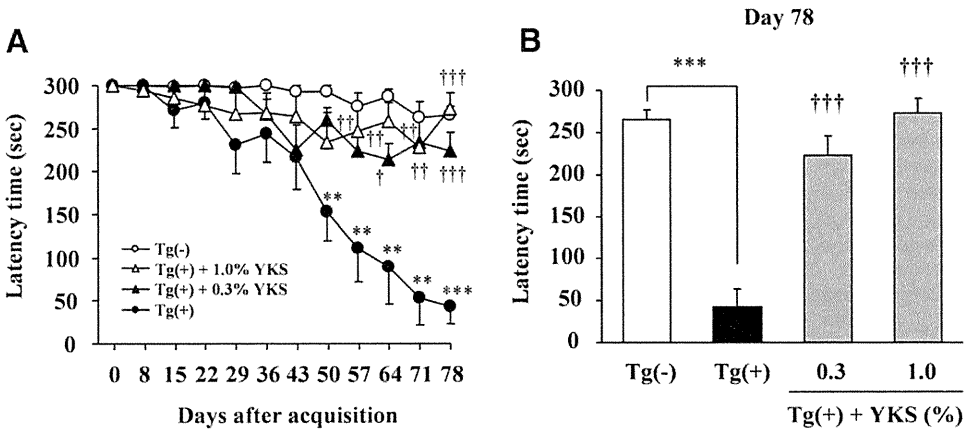

Fig. 2. Step-through latencies in the retention test of the passive-avoidance task in YKS-treated Tg mice. Changes in the latencies during retention tests for 78 d after acquisition of avoidance memory in each group are shown in (A), and the final results on day 78 are shown in (B). Values represent the means±SE (n=10 in each group). Significance by Mann-Whitney U test following analysis of variance (Kruskal-Wallis) is indicated as ** P<0.01, *** P<0.001 vs. corresponding Tg(−) control, and † P<0.05, †† P<0.01 and ††† P<0.001 vs. Tg(+) on each day.

groups acquired avoidance memory, staying in the illuminated compartment over 300 s on the fifth day. No statistically significant differences were observed in the mean latency times among all groups during the acquisition trials (data not shown).

Memory retention tests were performed once a week for 78 days after the final acquisition trial. Changes in the step-through latency in the YKS-treated groups are shown in Fig. 2A, and the results on the terminal day 78 are shown in Fig. 2B. The latency time of the Tg(+) group was significantly shorter than that of the Tg(−) group. The shorter latency was significantly prolonged by treatments with 0.3 and 1.0% YKS.

Changes in the step-through latency in UH-treated groups are shown in Fig. 3A, and then the results on the terminal day 78 are shown in Fig. 3B. The shortened latency time of the Tg(+) group was significantly prolonged by treatment with UH (0.1% and 1.0%) in a dose-dependent manner.

Effects of YKS and UH on aggressiveness and sociability in Tg(+) mice

The effects of YKS on aggressive behavior, social behavior, and motor activity are shown in Fig. 4. The aggressive behavior in the Tg(+) group increased significantly more than that in the Tg(−) group. The increase was significantly inhibited by treatment with 1.0% YKS (Fig. 4A). On the other hand, social behavior in the Tg(+) group decreased significantly more than that in the Tg(−) group. The decrease was significantly inhibited by treatment with 1.0% YKS (Fig. 4B). No significant differences of the motor activities (distance) were observed between Tg(−), Tg(+), and Tg(+)+YKS groups (Fig. 4C).

The effects of UH on aggressive behavior, social behavior, and motor activity are shown in Fig. 5. The aggressive behavior in the Tg(+) group increased significantly more than that in the Tg(−) group. The increase was

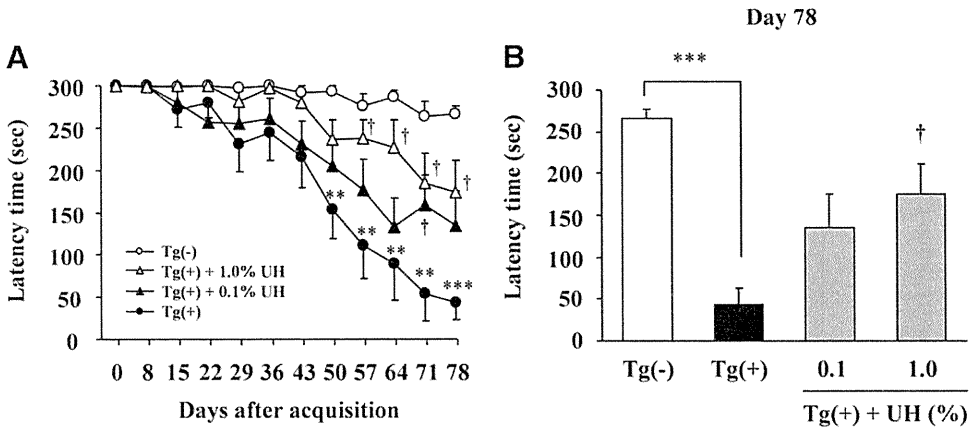

Fig. 3. Step-through latencies in the retention test of the passive-avoidance task in UH-treated Tg mice. Changes in the latencies during retention tests for 78 d after acquisition of avoidance memory in each group are shown in (A), and the final results on day 78 are shown in (B). All mice acquired avoidance memory by five repeated acquisition trials. Values represent the means±SE (n=10 in each group). Significance by Mann-Whitney U test following analysis of variance (Kruskal-Wallis) is indicated as ** P<0.01, *** P<0.001 vs. corresponding Tg(−) control, and † P<0.05 vs. Tg(+) on each day.

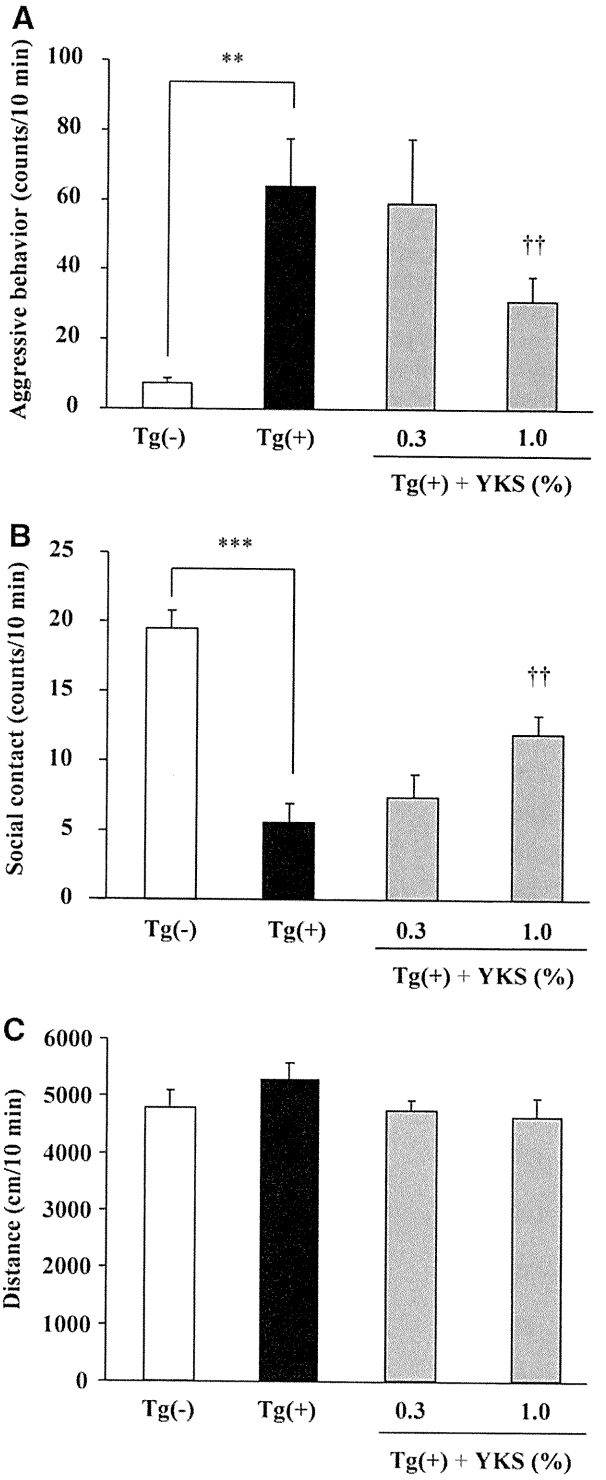

Fig. 4. Aggressive behavior (A), social contact (B), and distance as indexes of motor activity (C) of YKS-treated mice in the social interaction test. Value represents the mean±SE (n=10 in each group). Significance by Bonferroni/Dunn tests following one-way ANOVA is indicated as ** $P<0.01$, *** $P<0.001$ vs. Tg(−), and †† $P<0.01$ vs. Tg(+).

significantly inhibited by treatment with 1.0% UH (Fig. 5A). On the other hand, social behavior in the Tg(+) group decreased significantly more than that in the Tg(−) group. The decrease was significantly inhibited by treatment with 1.0% UH (Fig. 5B). No significant differences of the motor activities were observed between Tg(−), Tg(+), and Tg(+) + UH groups (Fig. 5C).

Effects of YKS and UH on cerebral Aβ levels in Tg(+) mice

To determine whether oral YKS or UH treatment affected the accumulation of Aβ in cerebral cortex, the cortical $A\beta_{1\text{-}40}$ and $A\beta_{1\text{-}42}$ levels were measured. The results are shown in Fig. 6A, B, respectively. Large amounts of both forms of Aβ were detected in the cortex of Tg(+) mice but not in Tg(−) mice. YKS or UH treatment had no significant effect on $A\beta_{1\text{-}40}$ levels in the Tg(+) mice (Fig. 6A). However, both YKS and UH inhibited $A\beta_{1\text{-}42}$ accumulation in Tg(+) mice in a dose-dependent manner (Fig. 6B).

DISCUSSION

Aβ is thought to be a causative substance of AD (Hsiao et al., 1996; Selkoe, 2002; Wirths et al., 2004). We previously demonstrated that UH (10 and 100 μg/ml) had a potent anti-aggregation effect on Aβ proteins *in vitro*, in a concentration-dependent manner (Fujiwara et al., 2006). In the present *in vitro* study, we demonstrated that YKS (100 μg/ml) significantly inhibited Aβ aggregation as shown in Fig. 1. UH is contained 14.6% in YKS, that is, 14.6 μg/ml of UH is contained in 100 μg/ml of YKS. This 14.6 μg/ml concentration is included within the range of effective concentrations (Fujiwara et al., 2006). Therefore, the anti-aggregation effect of YKS is suggested to be attributed to UH. It is important to verify whether *in vitro* results are reflected *in vivo*. However, it is difficult to compare effective dose or concentration directly between *in vitro* and *in vivo* experiments, because the experimental conditions are different between them. In the present *in vivo* study, YKS or UH were given to animals as diets containing 0.3 and 1.0% YKS, or 0.1 and 1.0% UH. The YKS intake levels in 0.3 and 1.0% YKS groups corresponded to 240 and 800 mg/kg/d when the levels were calculated from food consumption. Similarly, the UH intake levels in 0.1 and 1.0% UH groups corresponded to 80 and 800 mg/kg/d. As shown in Fig. 6B, we found that both YKS and UH dose-dependently inhibited $A\beta_{1\text{-}42}$ accumulation in the cerebral cortex of Tg(+) mice. As 800 mg/kg/d of YKS contains 117 mg/kg/d (14.6%) which is included within the range of 80 and 800 mg/kg/d of UH, we suggest the possibility that YKS (800 mg/kg/d) containing UH (117 mg/kg/d) has the anti-aggregation effect as well as the *in vitro* study. This is a first finding demonstrating that YKS and UH inhibit the accumulation of Aβ *in vivo*.

The Tg(+) mice used in the present study are known to develop disturbance of memory or cognitive function (Hsiao et al., 1996; Wegiel et al., 2001; Barnes et al., 2004; Ikarashi et al., 2004). In the present study, we evaluated the memory disturbance in Tg(+) mice using a step-through passive avoidance test. In the retention test, the latency time of the Tg(+) mice was significantly shorter

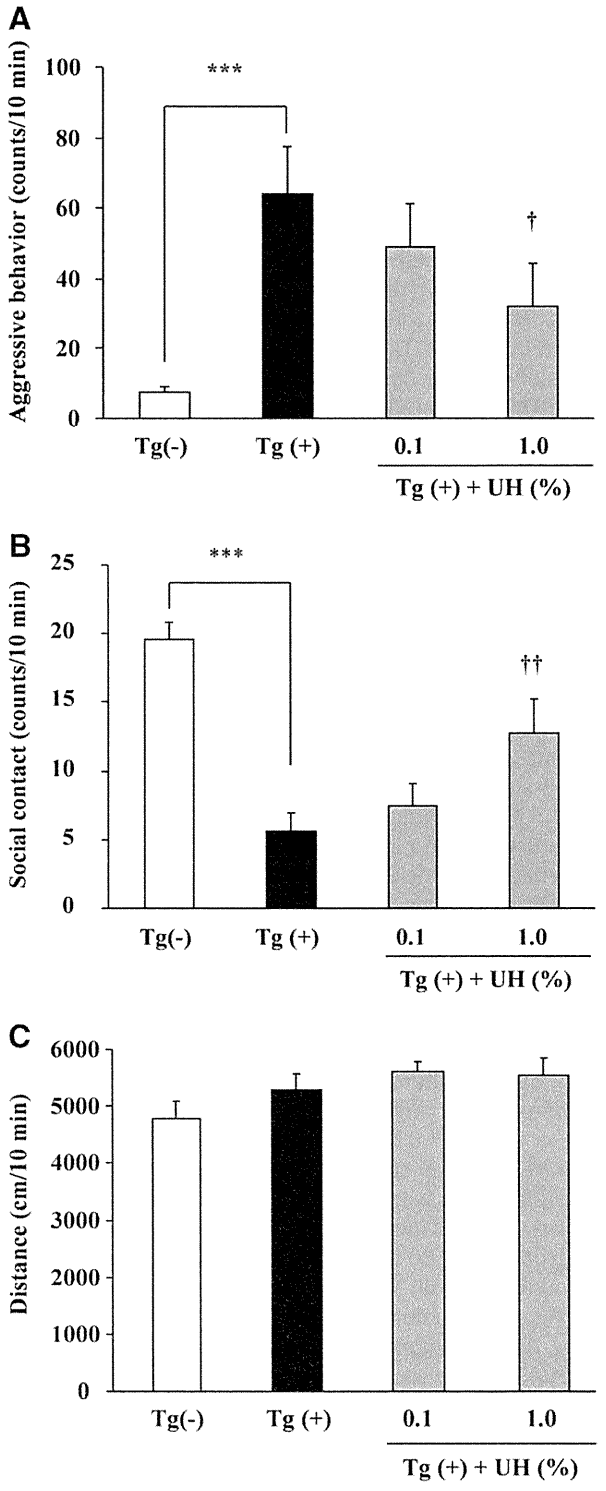

Fig. 5. Aggressive behavior (A), social contact (B), and distance as indexes of motor activity (C) of UH-treated mice in the social interaction test. Value represents the mean±SE (n=10 in each group). Significance by Bonferroni/Dunn tests following one-way ANOVA is indicated as *** P<0.001 vs. Tg(−), and † P<0.05, †† P<0.01 vs. Tg(+).

than that of the Tg(−) mice. The shorter latency in Tg(+) mice was significantly prolonged by treatment with YKS or UH. Though the prolongation of latency time is well-known to be affected by drug-dependent physical effects such as catalepsy and suppression of motor activity, we previously demonstrated that YKS did not induce them as haloperidol or risperidone does (Sekiguchi et al., 2009). Therefore, the ameliorative data of YKS and UH against the shorter latency in Tg(+) mice is thought to be not due to the physical disturbance, that is, these changes are selective to memory function, suggesting that YKS and UH might ameliorate the memory disturbance in Tg(+) mice.

Up till now, Tateno et al. (2008) demonstrated neuroprotective effects of YKS on Aβ-induced cytotoxicity in a primary culture of rat cortical neurons. We also recently demonstrated not only neuroprotective effects of YKS on glutamate-mediated excitotoxicity in cultured cells (Kawakami et al., 2009, 2010) but also ameliorative effects of YKS on learning and memory disturbance induced by i.c.v. injection of Aβ in mice (Sekiguchi et al., in press) and thiamine deficiency in rats (Ikarashi et al., 2009). These findings suggest that YKS has neuroprotective effects as one of the mechanisms. In addition to the mechanism, the

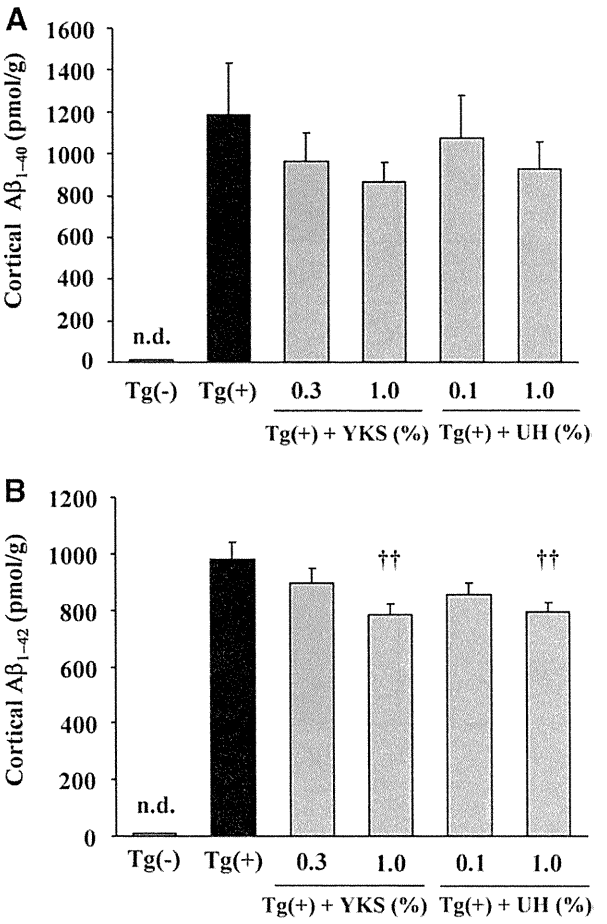

Fig. 6. Effects of YKS and UH on cortical concentrations of $A\beta_{1\text{-}40}$ (A) and $A\beta_{1\text{-}42}$ (B) in Tg mice. Large amounts of both forms of Aβ were detected in the cortex of Tg(+) mice but not in Tg(−) controls (n.d.). Values represent the mean±SE (n=10 in each group). Significance by Bonferroni/Dunn tests following one-way ANOVA is indicated as †† P<0.01 vs. Tg(+).

present results newly suggest a possibility that YKS ameliorates memory disturbance by preventing the aggregation of Aβ, which may be attributed to UH. To strongly support the participation of UH in the future, it will be necessary to confirm disappearance of the ameliorative effect of YKS by elimination of UH.

Kawarabayashi et al. (2001) demonstrated that Aβ deposit in the brain was started in the late stage (8–10 month old) though Aβ was detected biochemically in the early stage (4–5 month old). In the present study, YKS or UH was administered for 5 months from 10 to 15-month-old. In the acquisition trial for the learning at 11-month-old, no significant differences were observed in the latency times among all groups, suggesting that 11-month-old Tg(+) mice possess learning ability as well as Tg(−) control mice. However, the retention memory in the Tg(+) mice gradually decreased during 10- and 15-month-old during which Aβ deposits are facilitated. These data suggest close relation between Aβ deposit and memory disturbance. As YKS and UH ameliorated the memory disturbance in Tg(+) mice, these medicines are thought to have the preventing effect of memory disturbance.

On the other hand, in the present study, though it is true that YKS and UH statistically decreased Aβ accumulation, large amount of Aβ still existed in the brain: nevertheless, memory disturbance was ameliorated by treatment with YKS or UH. As a possible explanation for this ameliorative effect, synergistic effect of YKS including neuroprotective effect and inhibitory effect of Aβ aggregation is inferred. Furthermore, the improvement of cognition with YKS treatment was not demonstrated in clinical trials, most of which were evaluated in the comparatively short term of 4 weeks (Iwasaki et al., 2005a; Mizukami et al., 2009). To prove our hypothesis in the clinical trial, a long-term trial will be necessary in the future.

In patients with dementia, not only core symptoms but also BPSD often emerge. YKS has been reported to ameliorate BPSD such as hallucinations, agitation, and aggression in patients with AD, DLB, and other forms of senile dementia (Iwasaki et al., 2005a,b; Mizukami et al., 2009; Shinno et al., 2007, 2008). In the present study, the development of BPSD-like behaviors such as a marked increase in aggressive behavior and decrease in social behavior was observed in the Tg(+) mice, and YKS or UH ameliorated those abnormal behaviors. These effects, evaluated using social interaction tests, also are known to be influenced by changes in drug-dependent motor activity. In this test, we measured the traveling distance as an index of motor activity together with the interactive behavior, and confirmed that no significant difference in motor activity was observed among all groups. Therefore, the amelioration of aggression and sociability by YKS and UH are suggested to be a direct effect, not due to the secondary effect induced by the suppression of motor activity. The ameliorative effects by YKS of abnormal aggressiveness and sociability in Tg(+) mice are thought to support the finding in the clinical studies reporting that YKS ameliorated excitement, anger and decrease in activities of daily living in patients with AD (Iwasaki et al., 2005a).

Two mechanisms are inferred from the BPSD-ameliorating effect of YKS. One putative mechanism is that the effect may be obtained by inhibiting Aβ accumulation, which has already been discussed. However, it might be difficult to demonstrate this possibility by clinical studies because several clinical studies that evaluated YKS with a 4-week treatment period showed improvement in BPSD without amelioration of cognitive dysfunction in patients with dementia (Iwasaki et al., 2005a; Mizukami et al., 2009). This finding suggests another mechanism or possibility that YKS has a quicker improving effect on some neuronal function than the putative ameliorative effect on memory dysfunction and Aβ accumulation. Takeda et al. (2008a,b) reported that YKS attenuated the abnormal increase in cerebral glutamate release in zinc-deficient rats. Ikarashi et al. (2009) demonstrated YKS inhibited the increase in the cerebral extracellular concentration of glutamate in thiamine-deficient rats. Egashira et al. (2008) reported that YKS inhibited the 5-HT 2A receptor agonist-induced heat-twitch response by decreasing expression of 5-HT2A receptors in the prefrontal cortex. Terawaki et al. (2010) demonstrated *in vitro* that YKS and UH showed a partial agonistic effect on 5-HT1A receptors. This *in vitro* finding was also supported by *in vivo* experiment demonstrating that YKS ameliorated abnormal aggressiveness and sociability observed in para-chloroamphetamine-induced cerebral 5-HT-depletion rats, and the ameliorative effect was counteracted by co-administration of a 5-HT1A receptor antagonist, WAY-100635 (Kanno et al., 2009). Taken together, the ameliorative effects of YKS and UH on abnormal aggressive and social behaviors in Tg(+) mice may also relate to the glutamateric and serotonergic functions.

YKS has been used in Asian countries as a remedy for restlessness and agitation in children since it was developed by Xue Kai in 1555 (Iwasaki et al., 2005a). Recently, approximately over 100 million packages of YKS were sold during a year in Japan. Recent accumulated clinical studies reported not only the usefulness of YKS on BPSD but also information on the side effects. Mizukami et al. (2009) reported the appearance of hypokalaemia (two patients), gastrointestinal symptoms including vomiting/diarrhoea, nausea, epigastric distress (three patients), sedation (one patient), and leg edema (one patient) in a randomized cross-over study of YKS using 106 patients with dementia. In particular, the kampo medicines including glycyrrhiza, such as YKS, have been well-known to sometimes cause hypokalaemia (Ohtake et al., 2007; Makino et al., 2008). Therefore, the serum potassium concentration should be monitored.

CONCLUSION

In conclusion, the present study demonstrated that YKS inhibited accumulation of Aβ fibrils *in vitro* and *in vivo*. As a result, it improved not only memory deficits but also BPSD-like behaviors such as increased aggressive behavior and decreased social behavior in the APP transgenic

mice. Therefore, YKS may have potential as a therapeutic drug for patients with AD and mild cognitive impairment.

Acknowledgments—This work was partially supported by (1) a grant-in-aid for scientific research from the Ministry of Education, Science, Sports and Culture of Japan (#16590554), (2) a program for the promotion of fundamental studies in Health Science of the National Institute of Biomedical Innovation (NIBIO) of Japan (#03-1) and (3) a grant-in-aid from Core Research for Evolutional Science and Technology of Japan Science and Technology Corporation.

REFERENCES

Adriani W, Ognibene E, Heuland E, Ghirardi O, Caprioli A, Laviola G (2006) Motor impulsivity in APP-SWE mice: a model of Alzheimer's disease. Behav Pharmacol 17:525–533.

Barghorn S, Nimmrich V, Striebinger A, Krantz C, Keller P, Janson B, Bahr M, Schmidt M, Bitner RS, Harlan J, Barlow E, Ebert U, Hillen H (2005) Globular amyloid β-peptide$_{1-42}$ oligomer—a homogenous and stable neuropathological protein in Alzheimer's disease. J Neurochem 95:834–847.

Barnes P, Hale G, Good M (2004) Intramaze and extramaze cue processing in adult APP$_{SWE}$ Tg2576 transgenic mice. Behav Neurosci 118:1184–1195.

Barrow CJ, Zagorski MG (1991) Solution structures of beta peptide and its constituent fragments: relation to amyloid deposition. Science 253:179–182.

Calon F, Lim GP, Yang F, Morihara T, Teter B, Ubeda O, Rostaing P, Triller A, Salem N, Ashe KH, Frautschy SA, Cole GM (2004) Docosahexaenoic acid protects from dendritic pathology in an Alzheimer's disease mouse model. Neuron 43:633–645.

Darreh-Shori T, Hellström-Lindahl E, Flores-Flores C, Guan ZZ, Soreq H, Nordberg A (2004) Long-lasting acetylcholinesterase splice variations in anticholinesterase-treated Alzheimer's disease patients. J Neurochem 88:1102–1113.

Dong H, Csernansky CA, Martin MV, Bertchume A, Vallera D, Csernansky JG (2005) Acetylcholinesterase inhibitors ameliorate behavioral deficits in the Tg2576 mouse model of Alzheimer's disease. Psychopharmacology 181:145–152.

Egashira N, Iwasaki K, Ishibashi A, Hayakawa K, Okuno R, Abe M, Uchida N, Mishima K, Takasaki K, Nishimura R, Oishi R, Fujiwara M (2008) Repeated administration of Yokukansan inhibits DOI-induced head-twitch response and decreases expression of 5-hydroxytryptamine (5-HT)$_{2A}$ receptors in the prefrontal cortex. Prog Neuropsychopharmacol Biol Psychiatry 32:1516–1520.

File SE (1980) The use of social interaction as a method for detecting anxiolytic activity of chlordiazepoxide-like drugs. J Neurosci Methods 2:219–238.

Fujiwara H, Iwasaki K, Furukawa K, Seki T, He M, Maruyama M, Tomita N, Kudo Y, Higuchi M, Saido TC, Maeda S, Takashima A, Hara M, Ohizumi Y, Arai H (2006) *Uncaria rhynchophylla*, a Chinese medicinal herb, has potent antiaggregation effects on Alzheimer's β-amyloid proteins. J Neurosci Res 84:427–433.

Hsiao K, Chapman P, Nilsen S, Eckman C, Harigaya Y, Younkin S, Yang F, Cole G (1996) Correlative memory deficits, Aβ elevation, and amyloid plaques in transgenic mice. Science 274:99–102.

Ikarashi Y, Harigaya Y, Tomidokoro Y, Kanai M, Ikeda M, Matsubara E, Kawarabayashi T, Kuribara H, Younkin SG, Maruyama Y, Shoji M (2004) Decreased level of brain acetylcholine and memory disturbance in APP$_{SW}$ mice. Neurobiol Aging 25:483–490.

Ikarashi Y, Iizuka S, Imamura S, Yamaguchi T, Sekiguchi K, Kanno H, Kawakami Z, Yuzurihara M, Kase Y, Takeda S (2009) Effects of Yokukansan, a traditional Japanese medicine, on memory disturbance and behavioral and psychological symptoms of dementia in thiamine-deficient rats. Biol Pharm Bull 32:1701–1709.

Iwasaki K, Kobayashi S, Chimura Y, Taguchi M, Inoue K, Cho S, Akiba T, Arai H, Cyong JC, Sasaki H (2004) A randomized, double-blind, placebo-controlled clinical trial of the Chinese herbal medicine "ba wei di huang wan" in the treatment of dementia. J Am Geriatr Soc 52:1518–1521.

Iwasaki K, Satoh-Nakagawa T, Maruyama M, Monma Y, Nemoto M, Tomita N, Tanji H, Fujiwara H, Seki T, Fujii M, Arai H, Sasaki H (2005a) A randomized, observer-blind, controlled trial of the traditional Chinese medicine Yi-Gan San for improvement of behavioral and psychological symptoms and activities of daily living in dementia patients. J Clin Psychiatry 66:248–252.

Iwasaki K, Maruyama M, Tomita N, Furukawa K, Nemoto M, Fujiwara H, Seki T, Fujii M, Kodama M, Arai H (2005b) Effects of the traditional Chinese herbal medicine Yi-Gan San for cholinesterase inhibitor-resistant visual hallucinations and neuropsychiatric symptoms in patients with dementia with Lewy bodies. J Clin Psychiatry 66:1612–1613.

Kanno H, Sekiguchi K, Yamaguchi T, Terawaki K, Yuzurihara M, Kase Y, Ikarashi Y (2009) Effect of yokukansan, a traditional Japanese medicine, on social and aggressive behaviour of para-chloroamphetamine-injected rats. J Pharm Pharmacol 61:1249–1256.

Kawakami Z, Kanno H, Ueki T, Terawaki K, Tabuchi M, Ikarashi Y, Kase Y (2009) Neuroprotective effects of yokukansan, a traditional Japanese medicine, on glutamate-mediated excitotoxicity in cultured cells. Neuroscience 159:1397–1407.

Kawakami Z, Ikarashi Y, Kase Y (2010) Glycyrrhizin and its metabolite 18β-glycyrrhetinic acid in glycyrrhiza, a constituent herb of yokukansan, ameliorate thiamine deficiency-induced dysfunction of glutamate transport in cultured rat cortical astrocytes. Eur J Pharmacol 626:154–158.

Kawarabayashi T, Younkin LH, Saido TC, Shoji M, Ashe KH, Younkin SG (2001) Age-dependent changes in brain, CSF, and plasma amyloid (beta) protein in the Tg2576 transgenic mouse model of Alzheimer's disease. J Neurosci 21(2):372–381.

Lalonde R, Lewis TL, Strazielle C, Kim H, Fukuchi K (2003) Transgenic mice expressing the βAPP695SWE mutation: effects on exploratory activity, anxiety, and motor coordination. Brain Res 977: 38–45.

Makino T, Ohtake N, Watanabe A, Tsuchiya N, Imamura S, Iizuka S, Inoue M, Mizukami H (2008) Down-regulation of a hepatic transporter multidrug resistance-associated protein 2 is involved in alteration of pharmacokinetics of Glycyrrhizin and its metabolites in a rat model of chronic liver injury. Drug Metab Dispos 36: 1438–1443.

Maruyama M, Tomita N, Iwasaki K, Ootsuki M, Matsui O, Nemoto M, Okamura N, Higuchi M, Tsutsui M, Suzuki T, Seki T, Kaneta T, Furukawa K, Arai H (2006) Benefits of combining donepezil plus traditional Japanese herbal medicine on cognition and brain perfusion in Alzheimer's disease: a 12-week observer-blind, donepezil monotherapy controlled trial. J Am Geriatr Soc 54:869–871.

Millard CB, Broomfield CA (1995) Anticholinesterases: medical applications of neurochemical principles. J Neurochem 64:1909–1918.

Mizukami K, Asada T, Kinoshita T, Tanaka K, Sonohara K, Nakai R, Yamaguchi K, Hanyu H, Kanaya K, Takao T, Okada M, Kudo S, Kotoku H, Iwakiri M, Kurita H, Miyamura T, Kawasaki Y, Omori K, Shiozaki K, Odawara T, Suzuki T, Yamada S, Nakamura Y, Toba K (2009) A randomized cross-over study of a traditional Japanese medicine (kampo), yokukansan, in the treatment of the behavioural and psychological symptoms of dementia. Int J Neuropsychopharmacol 12:191–199.

Nagaratnam N, Lewis-Jones M, Scott D, Palazzi L (1998) Behavioral and psychiatric manifestations in dementia patients in a community: caregiver burden and outcome. Alzheimer Dis Assoc Disord 12:330–334.

Nakagawasai O, Yamadera F, Iwasaki K, Arai H, Taniguchi R, Tan-no K, Sasaki H, Tadano T (2004) Effect of kami-untan-to on the impairment of learning and memory induced by thiamine-deficient feeding in mice. Neuroscience 125:233–241.

Ognibene E, Middei S, Daniele S, Adriani W, Ghirardi O, Caprioli A, Laviola G (2005) Aspects of spatial memory and behavioral disin-

hibition in Tg2576 transgenic mice as a model of Alzheimer's disease. Behav Brain Res 156:225–232.

Ohtake N, Kido A, Kubota K, Tsuchiya N, Morita T, Kase Y, Takeda S (2007) A possible involvement of 3-monoglucuronyl-glycyrrhetinic acid, a metabolite of glycyrrhizin (GL), in GL-induced pseudoaldosteronism. Life Sci 80:1545–1552.

Park CH, Lee YJ, Lee SH, Choi SH, Kim HS, Jeong SJ, Kim SS, Suh YH (2000) Dehydroevodiamine. HCl prevents impairment of learning and memory and neuronal loss in rat models of cognitive disturbance. J Neurochem 74:244–253.

Quinn JF, Bussiere JR, Hammond RS, Montine TJ, Henson E, Jones RE, Stackman RW (2007) Chronic dietary α-lipoic acid reduces deficits in hippocampal memory of aged Tg2576 mice. Neurobiol Aging 28:213–225.

Sekiguchi K, Yamaguchi T, Tabuchi M, Ikarashi Y, Kase Y (2009) Effect of yokukansan, a traditional Japanese medicine, on aggressiveness induced by intracerebroventicular injection of amyloid β protein into mice. Phytother Res 23:1175–1181.

Sekiguchi K, Imamura S, Yamaguchi T, Tabuchi M, Kanno H, Terawaki K, Kase Y, Ikarashi Y (in press) Effect of yokukansan and donepezil on learning disturbance and aggressiveness induced by intracerebroventicular injection of amyloid β protein in mice. Phytother Res. Published online in Wiley Online Library (http://wileyonlinelibrary.com) DOI: 10.1002/ptr.3287.

Selkoe DJ (2002) Alzheimer's disease is a synaptic failure. Science 298:789–791.

Shinno H, Utani E, Okazaki S, Kawamukai T, Yasuda H, Inagaki T, Horiguchi J (2007) Successful treatment with Yi-Gan San for psychosis and sleep disturbance in a patient with dementia with Lewy bodies. Prog Neuro-Psychopharmacol Biol Psychiatry 31:1543–1545.

Shinno H, Inami Y, Inagaki T, Nakamura Y, Horiguchi J (2008) Effect of Yi-Gan San on psychiatric symptoms and sleep structure at patients with behavioral and psychological symptoms of dementia. Prog Neuropsychopharmacol Biol Psychiatry 32:881–885.

Stackman RW, Eckenstein F, Frei B, Kulhanek D, Nowlin J, Quinn JF (2003) Prevention of age-related spatial memory deficits in a transgenic mouse model of Alzheimer's disease by chronic *Ginkgo biloba* treatment. Exp Neurol 184:510–520.

Suemoto TA, Okamura N, Shiomitsu T, Suzuki M, Shimadzu H, Akatsu H, Yamamoto T, Kudo Y, Sawada T (2004) *In vivo* labeling of amyloid with BF-108. Neurosci Res 48:65–74.

Takeda A, Itoh H, Tamano H, Yuzurihara M, Oku N (2008a) Suppressive effect of yokukansan on excessive release of glutamate and aspartate in the hippocampus of zinc-deficient rats. Nutr Neurosci 11:41–46.

Takeda A, Tamano H, Itoh H, Oku N (2008b) Attenuation of abnormal glutamate release in zinc deficiency by zinc and yokukansan. Neurochem Int 53:230–235.

Tanji H, Ootsuka M, Matsui T, Maruyama M, Nemoto M, Tomita N, Seki T, Iwasaki K, Arai H, Sasaki H (2005) Dementia caregivers' burdens and use of public services. Geriatr Gerontol Int 5:94–98.

Tateno M, Ukai W, Ono T, Saito S, Hashimoto E, Saito T (2008) Neuroprotective effects of Yi-Gan San against beta amyloid-induced cytotoxicity on rat cortical neurons. Prog Neuropsychopharmacol Biol Psychiatry 32:1704–1707.

Terawaki K, Ikarashi Y, Sekiguchi K, Nakai Y, Kase Y (2010) Partial agonistic effect of yokukansan on human recombinant serotonin 1A receptors expressed in the membranes of Chinese hamster ovary cells. J Ethnopharmacol 127:306–312.

Tierney MC, Fisher RH, Lewis AJ, Zorzitto ML, Snow WG, Reid DW, Nieuwstraten P (1988) The NINCDS-ADRDA Work Group criteria for the clinical diagnosis of probable Alzheimer's disease: a clinicopathologic study of 57 cases. Neurology 38:359–364.

Wang Q, Iwasaki K, Suzuki T, Arai H, Ikarashi Y, Yabe T, Toriizuka K, Hanawa T, Yamada H, Sasaki H (2000) Potentiation of brain acetylcholine neurons by Kami-Untan-To (KUT) in aged mice: implications for a possible antidementia drug. Phytomedicine 7: 253–258.

Wegiel J, Wang KC, Imaki H, Imaki H, Rubenstein R, Wronska A, Osuchowski M, Lipinski WJ, Walker LC, LeVine H (2001) The role of microglial cells and astrocytes in fibrillar plaque evolution in transgenic APP_{SW} mice. Neurobiol Aging 22:49–61.

Wirths O, Multhaup G, Bayer TA (2004) A modified beta-amyloid hypothesis: intraneuronal accumulation of the beta-amyloid peptide—the first step of a fatal cascade. J Neurochem 91: 513–520.

(Accepted 31 January 2011)
(Available online 12 February 2011)

doi:10.1093/brain/awr038

BRAIN
A JOURNAL OF NEUROLOGY

^{18}F-THK523: a novel *in vivo* tau imaging ligand for Alzheimer's disease

Michelle T. Fodero-Tavoletti,[1,2] Nobuyuki Okamura,[3] Shozo Furumoto,[3] Rachel S. Mulligan,[4] Andrea R. Connor,[1,2] Catriona A. McLean,[5] Diana Cao,[6] Angela Rigopoulos,[6] Glenn A. Cartwright,[6] Graeme O'Keefe,[4] Sylvia Gong,[4] Paul A. Adlard,[1,7] Kevin J. Barnham,[1,2,7] Christopher C. Rowe,[4] Colin L. Masters,[7] Yukitsuka Kudo,[8] Roberto Cappai,[1,2] Kazuhiko Yanai[3] and Victor L. Villemagne[4,7]

1 Department of Pathology, The University of Melbourne, Victoria, 3010, Australia
2 Bio21 Molecular and Biotechnology Institute, The University of Melbourne, Victoria, 3010, Australia
3 Department of Pharmacology, Graduate School of Medicine, Tohoku University, Sendai, 980-8575, Japan
4 Department of Nuclear Medicine and Centre for PET, University of Melbourne, Austin Health, Victoria, 3084, Australia
5 Department of Anatomical Pathology, The Alfred Hospital, Victoria, 3181, Australia
6 Ludwig Institute for Cancer Research, Austin Hospital, Victoria, 3084, Australia
7 The Mental Health Research Institute, Victoria, 3010, Australia
8 Innovation of New Biomedical Engineering Centre, Tohoku University, Sendai, 980-8575, Japan

Correspondence to: Victor L. Villemagne,
Austin Health, Department of Nuclear Medicine and Centre for PET,
145 Studley Road,
Heidelberg,
VIC, 3084, Australia
E-mail: villemagne@petnm.unimelb.edu.au

While considerable effort has focused on developing positron emission tomography β-amyloid imaging radiotracers for the early diagnosis of Alzheimer's disease, no radiotracer is available for the non-invasive quantification of tau. In this study, we detail the characterization of ^{18}F-THK523 as a novel tau imaging radiotracer. *In vitro* binding studies demonstrated that ^{18}F-THK523 binds with higher affinity to a greater number of binding sites on recombinant tau (K18Δ280K) compared with β-amyloid$_{1-42}$ fibrils. Autoradiographic and histofluorescence analysis of human hippocampal serial sections with Alzheimer's disease exhibited positive THK523 binding that co-localized with immunoreactive tau pathology, but failed to highlight β-amyloid plaques. Micro-positron emission tomography analysis demonstrated significantly higher retention of ^{18}F-THK523 (48%; $P < 0.007$) in tau transgenic mice brains compared with their wild-type littermates or APP/PS1 mice. The preclinical examination of THK523 has demonstrated its high affinity and selectivity for tau pathology both *in vitro* and *in vivo*, indicating that ^{18}F-THK523 fulfils ligand criteria for human imaging trials.

Keywords: tau; imaging; Alzheimer's disease; dementia; PET
Abbreviations: PiB = Pittsburgh Compound-B

Introduction

The clinical diagnosis of neurodegenerative diseases such as Alzheimer's disease is typically based on progressive cognitive impairments while excluding other diseases. However, clinical diagnosis is often challenging, with patients presenting with mild and non-specific symptoms attributable to diverse and overlapping pathologies that present as similar phenotypes (van der Zee *et al.*,

Received September 23, 2010. Revised December 21, 2010. Accepted January 10, 2011